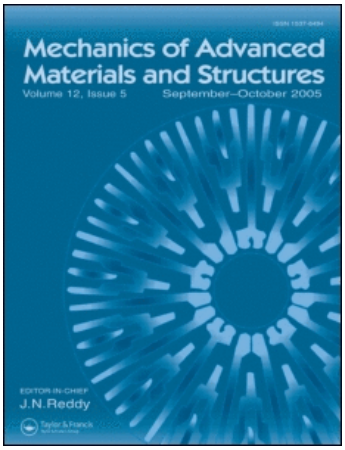

Mechanics of Advanced Materials and Structures
Publication details, including instructions for authors and subscription information:
http://www.informaworld.com/smpp/title~content=t713773278

The Generalized Method of Cells and High-Fidelity Generalized Method of Cells Micromechanical Models—A Review

Jacob Aboudi[a]
[a] Department of Solid Mechanics, Materials, and Systems, Faculty of Engineering, Tel-Aviv University, Ramat-Aviv, Israel

Online publication date: 12 August 2010

To cite this Article Aboudi, Jacob(2004) 'The Generalized Method of Cells and High-Fidelity Generalized Method of Cells Micromechanical Models—A Review', Mechanics of Advanced Materials and Structures, 11: 4, 329 — 366
To link to this Article: DOI: 10.1080/15376490490451543
URL: http://dx.doi.org/10.1080/15376490490451543

Mechanics of Advanced Materials and Structures, 11: 329–366, 2004

ISSN: 1537-6494 print / 1537-6532 online
DOI: 10.1080/15376490490451543

Taylor & Francis
Taylor & Francis Group

The Generalized Method of Cells and High-Fidelity Generalized Method of Cells Micromechanical Models—A Review

JACOB ABOUDI

Department of Solid Mechanics, Materials, and Systems, Faculty of Engineering, Tel-Aviv University, Ramat-Aviv, Israel

ABSTRACT

The models of the generalized method of cells and the recently developed high-fidelity generalized method of cells are reviewed. These two methods are micromechanical theories that are capable of providing the overall behavior of periodic multiphase materials of various types, including thermoelastic, viscoelastic, thermo-inelastic, and electromagnetothermoelastic materials. Both infinitesimal and finite deformation analyses of multiphase composites are discussed.

§1. INTRODUCTION

Micromechanical analyses provide the overall behavior of a multiphase material by taking into account the response of the individual constituents, their volume fractions, and the detailed interaction between the phases. A review of various micromechanical models can be found in the monographs by Aboudi [1] and Nemat-Nasser and Hori [2], for example. In this paper, the generalized method of cells (GMC) (from which its precursor, the method of cells (MOC), is obtained as a special case) and the most recent generalization, referred to as the high-fidelity generalized method of cells (HFGMC), are reviewed. Both the MOC and GMC have been reviewed by Aboudi [3]; hence, papers written after 1996 by various researchers that employed these methods will be reviewed.

In Section 2, the GMC is discussed together with the resulting constitutive laws for thermo-inelastic composites with one-way and two-way thermomechanical coupling, and its application by various researchers is reviewed. Section 3 presents the application of GMC for the modeling of smart multiphase materials. These include electromagnetic, electrostrictive, and shape-memory alloy composites. In Section 4, the GMC is applied to predict the response of multiphase thermoelastic and viscoelastic materials that can sustain finite deformations. Finally, Section 5 presents the newly developed HFGMC micromechanical theory, which is based on the homogenization technique. It is applied to thermoelastic, thermo-inelastic, electromagnetic, and finitely deformed multiphase composites. In all cases applications of these approaches by various researchers are described.

Received 16 April 2002; accepted 18 July 2003.

The author gratefully acknowledges the support of the Diane and Arthur Belfer Chair of Mechanics and Biomechanics.

Address correspondence to Jacob Aboudi, Department of Solid Mechanics, Materials, and Systems, Faculty of Engineering, Tel-Aviv University, Ramat-Aviv, 69978 Israel. E-mail: aboudi@eng.tau.ac.il

Based on the GMC, the NASA Glenn Research Center developed a micromechanics computer code, referred to as MAC/GMC, that has many user-friendly features and significant flexibility for the analysis of continuous, discontinuous, and woven polymer, ceramic, and metal matrix composites with phases that can be represented by arbitrary elastic, viscoelastic, and/or viscoplastic constitutive models. The most recent version of a user guide to this code (version 4) which has been presented by Bednarcyk and Arnold [4], incorporates HFGMC, together with additional material models including smart materials (electromagnetic and shape memory alloys) and yield surface prediction of metal matrix composites.

§2. The generalized method of cells

The article by Aboudi [5] is the first paper in which elements of the MOC can be detected. It deals with wave propagation in elastic fiber-reinforced composites. The prediction of the overall behavior of elastic-viscoplastic unidirectional composites by MOC appeared in [6]. The use of the MOC to predict various types of composites appeared in several papers, which have been summarized in a monograph by Aboudi [1]. The number of different phases of a composite that the MOC was able to analyze was limited to four, but the GMC theory [7, 8] extends the model to any number of phases, rendering a micromechanical model for multiphase materials. This generalization extends the modeling capability of the MOC to include the following:

- inelastic thermomechanical response of multiphase, metal matrix composites;
- modeling of various fiber shapes (architectures) by approximating the fiber inclusion by a suitable assemblage of subcells;
- analysis of different fiber arrays (packing or distributions);
- modeling of porosities and damage; and
- modeling of interfacial regions around inclusions, including interfacial degradation.

The basic micromechanical GMC analysis consists of four steps as follows:

1. The repeating unit cell for a given fiber shape and array in the periodic composite is identified, see Figure 1*a*, which displays a periodic multiphase material, described with respect to the global coordinates $\mathbf{x} = (x_1, x_2, x_3)$. Figure 1*b* shows the repeating unit cell defined with respect to local coordinates $\mathbf{y} = (y_1, y_2, y_3)$. The repeating unit cell is divided into $N_p N_q N_r$ rectangular parallelepiped generic cells. A typical generic cell, labeled as (p, q, r) with the running indices $p = 1, \ldots, N_p; q = 1, \ldots, N_q$; and $r = 1, \ldots, N_r$ in the three orthogonal directions, respectively, is shown in Figure 1*c*. It consists of eight subcells, every one of which is denoted by $(\alpha\beta\gamma)$ where $\alpha, \beta, \gamma = 1, 2$. Thus, the total number of subcells in the repeating unit cell is $8N_pN_qN_r$. The volume of each subcell is $d_\alpha^{(p)} h_\beta^{(q)} l_\gamma^{(r)}$ and the volume of the repeating cell is DHL, where

$$D = \sum_{p=1}^{N_p} \left(d_1^{(p)} + d_2^{(p)}\right) \qquad H = \sum_{q=1}^{N_q} \left(h_1^{(q)} + h_2^{(q)}\right) \qquad L = \sum_{r=1}^{N_r} \left(l_1^{(r)} + l_2^{(r)}\right)$$

Any subcell $(\alpha\beta\gamma)$ can be filled in general by a thermo-inelastic material, the constitutive law of which is given by

$$\boldsymbol{\sigma}^{(\alpha\beta\gamma)} = \mathbf{C}^{(\alpha\beta\gamma)}\left[\boldsymbol{\epsilon}^{(\alpha\beta\gamma)} - \boldsymbol{\epsilon}^{I(\alpha\beta\gamma)} - \boldsymbol{\epsilon}^{T(\alpha\beta\gamma)}\right] \tag{1}$$

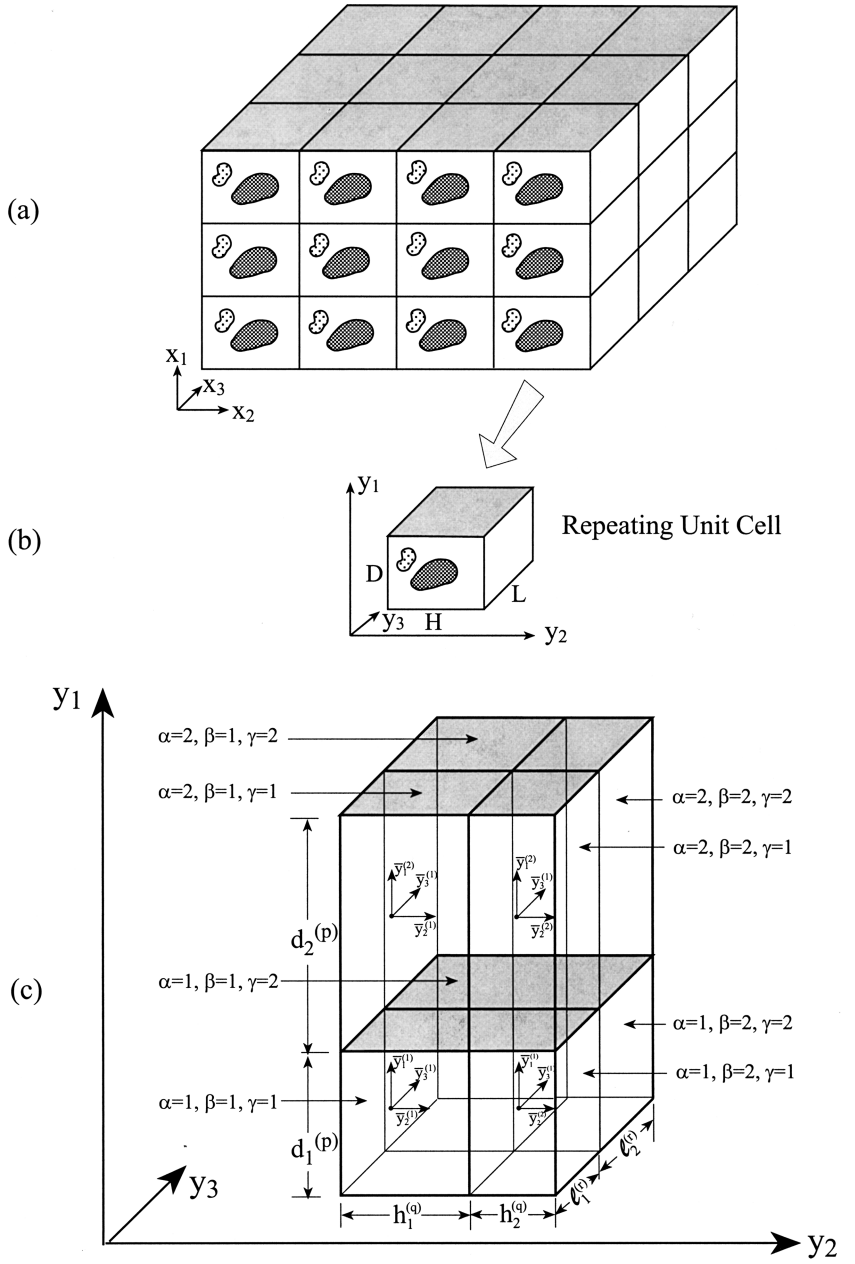

Figure 1. (a) *A multiphase composite with periodic microstructures.* (b) *The repeating unit cell.* (c) *A typical generic cell into several of which the repeating unit cell is discretized. The generic cell consists of eight subcells labeled as* $\alpha, \beta, \gamma = 1, 2$.

where $\boldsymbol{\sigma}^{(\alpha\beta\gamma)}$, $\boldsymbol{\epsilon}^{(\alpha\beta\gamma)}$, $\boldsymbol{\epsilon}^{I(\alpha\beta\gamma)}$, and $\boldsymbol{\epsilon}^{T(\alpha\beta\gamma)}$ are the stress, total strain, inelastic strain, and thermal strain tensors, respectively, and $\mathbf{C}^{(\alpha\beta\gamma)}$ is the stiffness tensor of the material filling the subcell.

2. The definition of the macroscopic average strains $\bar{\boldsymbol{\epsilon}}$ and stresses $\bar{\boldsymbol{\sigma}}$ from the corresponding microscopic average quantities in the subcells, $\bar{\boldsymbol{\epsilon}}^{(\alpha\beta\gamma)}$, $\bar{\boldsymbol{\sigma}}^{(\alpha\beta\gamma)}$

(homogenization), are

$$\bar{\boldsymbol{\epsilon}} = \frac{1}{DHL}\sum_{p=1}^{N_p}\sum_{q=1}^{N_q}\sum_{r=1}^{N_r}\sum_{\alpha,\beta,\gamma=1}^{2} d_\alpha^{(p)} h_\beta^{(q)} l_\gamma^{(r)} \bar{\boldsymbol{\epsilon}}^{(\alpha\beta\gamma)} \tag{2a}$$

$$\bar{\boldsymbol{\sigma}} = \frac{1}{DHL}\sum_{p=1}^{N_p}\sum_{q=1}^{N_q}\sum_{r=1}^{N_r}\sum_{\alpha,\beta,\gamma=1}^{2} d_\alpha^{(p)} h_\beta^{(q)} l_\gamma^{(r)} \bar{\boldsymbol{\sigma}}^{(\alpha\beta\gamma)} \tag{2b}$$

The basic assumption in MOC and GMC is that the displacement vector $\mathbf{u}^{(\alpha\beta\gamma)}$ in every subcell can be expanded linearly in terms of local coordinates $(\bar{y}_1^{(\alpha)}, \bar{y}_2^{(\beta)}, \bar{y}_3^{(\gamma)})$ located at the center of the subcell:

$$\mathbf{u}^{(\alpha\beta\gamma)} = \mathbf{W}_{(000)}^{(\alpha\beta\gamma)}(\mathbf{x}) + \bar{y}_1^{(\alpha)}\mathbf{W}_{(100)}^{(\alpha\beta\gamma)} + \bar{y}_2^{(\beta)}\mathbf{W}_{(010)}^{(\alpha\beta\gamma)} + \bar{y}_3^{(\gamma)}\mathbf{W}_{(001)}^{(\alpha\beta\gamma)} \tag{3}$$

where $\mathbf{W}_{(000)}^{(\alpha\beta\gamma)}$ is the displacement vector at the center of the subcell, and the other terms $\mathbf{W}_{(lmn)}^{(\alpha\beta\gamma)}$ characterize the linear dependence of the displacements on the local coordinates. These field quantities must be determined according to continuity of displacement and traction requirements.

3. Continuity of displacements and tractions is imposed at the interfaces between the constituents that fill the subcells, as well as between the repeating cells. These establish, in conjunction with microequilibrium, the relationships between the microscopic total, thermal and inelastic strains and macroscopic strains via the mechanical and thermal/inelastic concentration tensors (referred to as localization). For example, it can be shown [8] that for the GMC with the discontinuous fiber formulation the average strains $\bar{\boldsymbol{\epsilon}}^{(\alpha\beta\gamma)}$ in the subcells are given in terms of the macroscopic strains $\bar{\boldsymbol{\epsilon}}$ and the subcells' inelastic and thermal strains in the form

$$\bar{\boldsymbol{\epsilon}}^{(\alpha\beta\gamma)} = \mathbf{A}^{(\alpha\beta\gamma)}\bar{\boldsymbol{\epsilon}} + \mathbf{D}^{(\alpha\beta\gamma)}\left(\boldsymbol{\epsilon}_s^I + \boldsymbol{\epsilon}_s^T\right) \tag{4}$$

where $\mathbf{A}^{(\alpha\beta\gamma)}$, $\mathbf{D}^{(\alpha\beta\gamma)}$ are the appropriate concentration tensors and $\boldsymbol{\epsilon}_s^I$, $\boldsymbol{\epsilon}_s^T$ are the microscopic inelastic and thermal strains in all the subcells.

4. The resulting overall (macroscopic) constitutive equation of the multiphase composite is derived. The resulting composite thermo-inelastic constitutive law is obtained from the constitutive equations of the material in the subcell in conjunction with Eqs. (2*b*) and (4) as follows:

$$\bar{\boldsymbol{\sigma}} = \mathbf{C}^*(\bar{\boldsymbol{\epsilon}} - \bar{\boldsymbol{\epsilon}}^I - \bar{\boldsymbol{\epsilon}}^T) \tag{5}$$

In this constitutive equation $\mathbf{C}^*$ is the effective elastic stiffness tensor of the multiphase composite, which is given in terms of the elastic stiffnesses $\mathbf{C}^{(\alpha\beta\gamma)}$ of the constituents in a closed-form manner:

$$\mathbf{C}^* = \frac{1}{DHL}\sum_{p=1}^{N_p}\sum_{q=1}^{N_q}\sum_{r=1}^{N_r}\sum_{\alpha,\beta,\gamma=1}^{2} d_\alpha^{(p)} h_\beta^{(q)} l_\gamma^{(r)} \mathbf{C}^{(\alpha\beta\gamma)}\mathbf{A}^{(\alpha\beta\gamma)} \tag{6}$$

The resulting composite inelastic strain tensor in Eq. (5) has the following form:

$$\bar{\boldsymbol{\epsilon}}^I = \frac{-1}{DHL}\mathbf{C}^{*-1}\sum_{p=1}^{N_p}\sum_{q=1}^{N_q}\sum_{r=1}^{N_r}\sum_{\alpha,\beta,\gamma=1}^{2} d_\alpha^{(p)} h_\beta^{(q)} l_\gamma^{(r)} \mathbf{C}^{(\alpha\beta\gamma)}\left[\mathbf{D}^{(\alpha\beta\gamma)}\boldsymbol{\epsilon}_s^I - \bar{\boldsymbol{\epsilon}}^{I(\alpha\beta\gamma)}\right] \tag{7}$$

Similarly, the composite thermal strain tensor is given by

$$\bar{\boldsymbol{\epsilon}}^T = \frac{-1}{DHL}\mathbf{C}^{*-1}\sum_{p=1}^{N_p}\sum_{q=1}^{N_q}\sum_{r=1}^{N_r}\sum_{\alpha,\beta,\gamma=1}^{2} d_\alpha^{(p)} h_\beta^{(q)} l_\gamma^{(r)} \mathbf{C}^{(\alpha\beta\gamma)}\left[\mathbf{D}^{(\alpha\beta\gamma)}\boldsymbol{\epsilon}_s^T - \bar{\boldsymbol{\epsilon}}^{T(\alpha\beta\gamma)}\right] \tag{8}$$

In the special case of continuous fibers with four subcells consisting of perfectly elastic materials, the preceding analysis is given in detail in the textbook by Herakovich [9].

With ΔT denoting the temperature deviation from a reference temperature, the thermal strain tensor $\bar{\boldsymbol{\epsilon}}^T$ given by Eq. (8) readily provides the effective coefficients of thermal expansion $\boldsymbol{\alpha}^*$ of the multiphase composite according to

$$\boldsymbol{\alpha}^* = \bar{\boldsymbol{\epsilon}}^T/\Delta T$$

from which the effective thermal stress tensor $\boldsymbol{\Gamma}^*$ is obtained as $\boldsymbol{\Gamma}^* = \mathbf{C}^*\boldsymbol{\alpha}^*$.

It is also possible to use Levin's theorem [10], which directly provides the effective thermal stress vector $\boldsymbol{\Gamma}^*$ in terms of the individual thermal stress vectors $\boldsymbol{\Gamma}^{(\alpha\beta\gamma)}$ of the phases and the concentrations matrices $\mathbf{A}^{(\alpha\beta\gamma)}$ as follows

$$\bar{\boldsymbol{\Gamma}}^* = \frac{1}{DHL}\sum_{p=1}^{N_p}\sum_{q=1}^{N_q}\sum_{r=1}^{N_r}\sum_{\alpha,\beta,\gamma=1}^{2} d_\alpha^{(p)} h_\beta^{(q)} l_\gamma^{(r)} \mathbf{A}^{\mathrm{t}(\alpha\beta\gamma)}\boldsymbol{\Gamma}^{(\alpha\beta\gamma)} \tag{9}$$

where $\mathbf{A}^{\mathrm{t}(\alpha\beta\gamma)}$ denotes the transpose of $\mathbf{A}^{(\alpha\beta\gamma)}$. Both estimates of the effective thermal stress tensor obtained directly from the GMC model via Eq. (8), and Levin's expression, Eq. (9), coincide, implying the consistency of the GMC theory.

Because in the framework of GMC the stresses are constants at every subcell, it possible to employ Levin's theorem (just like Eq. (9)) and directly obtain the inelastic strain [11] in the form

$$\bar{\boldsymbol{\epsilon}}^I = \frac{1}{DHL}\sum_{p=1}^{N_p}\sum_{q=1}^{N_q}\sum_{r=1}^{N_r}\sum_{\alpha,\beta,\gamma=1}^{2} d_\alpha^{(p)} h_\beta^{(q)} l_\gamma^{(r)} \mathbf{Q}^{t(\alpha\beta\gamma)}\boldsymbol{\epsilon}^{I(\alpha\beta\gamma)} \tag{10}$$

where $\mathbf{Q}^{t(\alpha\beta\gamma)}$ denotes the transpose of the *mechanical* concentration tensors $\mathbf{Q}^{(\alpha\beta\gamma)}$ that connect the stress $\boldsymbol{\sigma}^{(\alpha\beta\gamma)}$ in the subcell to the average stress $\bar{\boldsymbol{\sigma}}$; that is,

$$\boldsymbol{\sigma}^{(\alpha\beta\gamma)} = \mathbf{Q}^{(\alpha\beta\gamma)}\bar{\boldsymbol{\sigma}} \tag{11}$$

It can be easily verified that

$$\mathbf{Q}^{(\alpha,\beta,\gamma)} = \mathbf{C}^{(\alpha\beta\gamma)}\mathbf{A}^{(\alpha\beta\gamma)}\mathbf{C}^{*-1} \tag{12}$$

As in the thermal case, it can be numerically verified that the overall inelastic strains provided by the GMC, Eq. (7), and closed-form expression (10) coincide. The corresponding GMC

analysis for continuous fibers reinforcing a viscoplastic matrix has been given by Paley and Aboudi [7] for both total and rate formulations.

The determination of the concentration tensors $\mathbf{A}^{(\alpha\beta\gamma)}$ requires the solution of a linear system of $48N_pN_qN_r$ algebraic equations in which the unknowns are the strain components in the subcells. Consequently, the computer time required for the inversion of this system can be significant as, for example, in the case of inelastic constituents with temperature-dependent properties, which necessitates an inversion at every step of the incremental procedure. As discussed by Pindera and Bednarcyk [12], due to the inherent lack of shear coupling between normal and shear stress and strain components within the GMC analysis it is possible to reduce dramatically the order of the algebraic system by employing the subcell stresses as unknowns (instead of the strains). This efficient reformulation of the GMC yields a system of $4(N_pN_q + N_pN_r + N_qN_r) + 2(N_p + N_q + N_r)$ algebraic equations, which is significantly smaller than the unreformulated system, especially as the number of subcells increases. As a result of this feature of the GMC, the computational efficiency of the model is significantly improved. Furthermore, in the analysis of a composite inelastic structure, the constitutive equations provided by the GMC (see Eq. (5)) are used repeatedly at every point of the structure. As a result, the dramatic advantage of this GMC reformulation is obvious.

In the previous development, one-way coupling between the mechanical and thermal effects in the constituent was assumed to exist (see Eq. (1)). In this situation the energy equation (heat equation) is uncoupled to the mechanical ones, and the temperature in the composite is uniform and can be imposed in advance. Williams and Aboudi [13] extended the micromechanical analysis to accommodate the case when there is a two-way thermo-mechanical coupling in the material that fills the subcell. Fully thermomechanical coupling occurs in all materials, and it arises due to the presence of both temperature and deformation effects in the energy equation and the equilibrium equations (through the constitutive relations). In this situation, the constitutive equations of the inelastic materials that fill the subcells are given by Eq. (1), whereas the energy equation that governs the temperature field distribution in the subcell $(\alpha\beta\gamma)$ is given by [14]

$$[\rho c_v \dot{T}]^{(\alpha\beta\gamma)} = [-\operatorname{div}\mathbf{q} + \zeta\boldsymbol{\sigma}\dot{\boldsymbol{\epsilon}}^I - T\boldsymbol{\Gamma}(\dot{\boldsymbol{\epsilon}} - \dot{\boldsymbol{\epsilon}}^I) + \rho\dot{R}]^{(\alpha\beta\gamma)} \tag{13}$$

where $\dot{}$ dot denotes a time derivative, $\rho^{(\alpha\beta\gamma)}$ is the material density, $c_v^{(\alpha\beta\gamma)}$ is the specific heat at constant volume, $\zeta^{(\alpha\beta\gamma)}$ is a partitioning factor for the inelastic work, $\dot{\boldsymbol{\epsilon}}^{I(\alpha\beta\gamma)}$ is the inelastic strain rate, $\dot{R}^{(\alpha\beta\gamma)}$ is an energy source term, and $\mathbf{q}^{(\alpha\beta\gamma)}$ is the thermal flux vector, which is given by the Fourier law

$$\mathbf{q}^{(\alpha\beta\gamma)} = -\boldsymbol{\kappa}_0^{(\alpha\beta\gamma)} \operatorname{grad} T^{(\alpha\beta\gamma)} \tag{14}$$

with $\kappa_0^{(\alpha\beta\gamma)}$ denoting the thermal conductivity tensor of the material.

2.1. *Applications*

The MOC and GMC have been employed by various investigators as is briefly described in the following.

Bennett and Haberman [15] adopted the MOC analysis to establish a micromechanical approach, which has been applied under various circumstances. They proposed to unify the finite element method and the MOC to provide a practical tool for including micromechanical effects in structural calculations.

Bednarcyk and Pindera [16] developed an analytical model based on the MOC and the classical lamination theory to investigate the effect of the matrix inelastic constitutive representation (classical plasticity and Freed et al. [17] viscoplasticity theory) and the effect of nonuniform fiber distribution on the thermal expansion of unidirectional graphite/copper composites.

An analytical solution has been presented by Williams and Pindera [18] for the prediction of the inelastic response of multilayered concentric cylinder assemblage subjected to axial shear loading. This solution forms a basis for the modeling of unidirectional metal matrix composites under axial shear loading. A comparison between this exact solution and the GMC prediction exhibits very good agreement.

By using the GMC for the prediction of the overall response of metal matrix composites, two mathematical models have been developed by Baxter and Pindera [19] for the thermal cooldown phase of composite fabrication. The first is a baseline model of idealized processing conditions, and the second model extends the first one by including a tooling constraint generally associated with fabrication techniques.

The modeling of the inelastic response of a porous, hybrid-fiber composite referred to as A–PA/IC50 has been considered by Roerden and Herakovich [20]. Its modeling requires three-step micromechanical analyses in which the GMC methodology has been successively implemented. The three steps include (1) analysis of a porous isotropic elastic alumina binder; (2) analysis of an anisotropic, elastic hybrid fiber (which is obtained by embedding Nextel 610 filaments in the porous binder); and (3) analysis of an anisotropic, inelastic metal matrix composite (which is obtained by adding IC50 nickel aluminide).

A recursive algorithm for the evaluation of elastic constants of uniaxially reinforced fiber composites with multiple coatings around the fiber has been developed by Upadhyay and Lyons [21]. Two concentric phases were considered at a time, and the effective elastic moduli were obtained from the MOC.

Mahiou and Béakou [22] investigated the effect of imperfect bonding between fibers and matrix in composites. To this end, they employed the MOC with a jump in displacement to model the fiber–matrix debonding. They also followed a second approach according to which the fiber and an interphase are replaced by an equivalent homogeneous medium.

Lissenden [23] introduced a fiber–matrix debonding model, based on Needleman's [24] cohesive zone interfacial representation, and implemented it in the MOC. The fiber–matrix interface is described by its strength and ductility. Coulombic frictional forces resist sliding after debonding initiates and complete interfacial separation occurs when the magnitude of the interfacial displacement exceeds the ductility of the interface.

In a series of papers, the MOC and GMC have been employed by Lissenden and Arnold [25, 26], Iyer et al. [27], and Lissenden et al. [28] for the study of the behavior of metal matrix composites. The authors present an innovative investigation of the initial and subsequent yield surfaces that have been generated by following two different approaches, namely, surfaces of constant inelastic strain rate and surfaces of constant dissipation rate. Furthermore, the effect of the existence of damage on the generated yield surfaces was presented. This damage is caused by the fiber–matrix debonding and has been modeled by a suitable representation that includes a Coulombian friction which involves a debonding initiation criterion. The effect of fiber architecture was investigated by considering rectangular, hexagonal, and square diagonal packing. The metallic matrix is represented by a generalized viscoplasticity with potential structure that includes nonlinear kinematic hardening with thermal and strain recovery mechanisms referred to as generalized viscoplasticity with potential structure (GVIPS) [29].

The effect of weak interfacial bonding on the tensile response of a titanium matrix composite was investigated by Goldberg and Arnold [30] by utilizing the GMC model. The fiber–matrix interface was modeled through application of a displacement discontinuity between fiber and matrix once a critical debonding stress had been exceeded.

Aghdam et al. [31] employed the MOC analysis for the prediction of initial yield, collapse, and gross plasticity envelopes of metal matrix composites subjected to various types of loadings and compared their analytical prediction with those provided by a finite element procedure.

A two-dimensional woven fabric composite strength model has been presented by Naik and Ganesh [32, 33] for the prediction of the failure strength of two-dimensional orthogonal plain-weave fabric laminates subjected to in-plane shear and uniaxial tensile loading. To this end, these authors used the MOC to determine the effective properties of the fiber-reinforced composite and the developed subcell stresses.

A new representation of the tensile failure of composite materials has been developed by Mahiou and Béakou [34] that accounts for the normal stress supported by the matrix and allows a study of the influence of the constituent material properties and fiber volume fraction on the stress concentration factors. To this end, they used the MOC, which provides the relation between the local states of stress and strain in the fiber and matrix phases and the applied stress and strain on the composite.

Robertson and Mall [35] utilized the MOC to analyze the behavior of metal matrix composites in the presence of fiber fragmentation. The inclusion of fiber damage effects has been accomplished by determining an equivalent fiber modulus based on the chain-of-bundles' fiber fragmentation analysis of Curtin [36].

The prediction of failure of longitudinally reinforced composites has been addressed by Bednarcyk and Arnold [37]. They considered two models to account for fiber breakage. The first is Curtin's effective fiber breakage model [38], and the second is a newly developed discrete model that considers failure of many individual fibers in a repeating unit cell of the composite. This model is based on the GMC methodology and explicitly includes the important feature of local stress unloading in fractured fibers, even as global loading of the composite continues.

Bednarcyk and Arnold [39] considered local interfacial debonding in composites. They developed, in conjuction with GMC analysis, a new model that allows debonding to progress via unloading of interfacial stresses even as global loading of the composite continues.

A micromechanical approach to model the fatigue life of a metal matrix composite has been proposed by Foringer et al. [40]. This was accomplished by combining the unified viscoplasticity theory with directional hardening of Bodner-Partom [41], with a micromechanical analysis based on the MOC and a damage accumulation model.

The MOC has also been employed by Fleming and Dowson [42] to predict the fatigue life of a metal matrix composite by assuming that the matrix material in the composite fails at the same fatigue stress level as the monolithic material or, if fibers fail, this will be at the failure level of the individual fibers.

A micromechanical failure analysis has been carried out by Wilt et al. [43]. It is based on the GMC micromechanical approach in which the multiaxial, isothermal, continuum damage mechanics model of Arnold and Kruch [44] has been incorporated.

More recently, the deformation, failure, and low cycle fatigue life of a metal matrix composite have been predicted by Bednarcyk and Arnold [45] by using a coupled deformation and damage approach in conjunction with the GMC micromechanical model. The local effects of inelastic deformation, fiber breakage, fiber–matrix interfacial debonding, and

fatigue damage are included. In addition, the lamination theory is employed as the structural scale in which GMC is embedded to operate on the mesoscale, between the global scale of the laminate and the microscale of the individual phases, to simulate the behavior of the composite material within each layer.

Continuum damage has been incorporated into the GMC by Voyiadjis and Deliktas [46] and applied to metal matrix composites. The local incremental damage model of Voyiadjis and Guelzim [47] has been used to account for damage in each subcell separately. The resulting GMC micromechanical analysis establishes elastoplastic constitutive equations that govern the overall behavior of the composite with evolving damage. More detailed discussions can be found in the book by Voyiadjis and Kattan [48] where a chapter is devoted to the GMC analysis which includes continuum damage.

The GMC has been applied by Reynolds and Baxter [49] to model the hardening behavior of strengthened 8009 aluminum alloy. The behavior of the multiphase material under monotonic loading and fully reversed loading has been investigated by comparing the model prediction with measured data.

The influence of pore geometry on the effective properties of porous materials has been investigated by Herakovich and Baxter [50] by utilizing the GMC model. Four distinct pore geometries have been studied and the predicted effective elastic properties have been compared with several results from other available models and measured data.

There are only few investigations in the literature concerning the micromechanical prediction of the behavior of discontinuously reinforced inelastic composites, because the study of short-fiber composites requires a three-dimensional analysis which is certainly highly intensive and more complicated. Pahr and Arnold [51] presented an extensive micromechanical investigation of the behavior of discontinuously reinforced composites using the GMC model. By performing numerous comparisons with finite element solutions and bound estimates, these authors showed that, whereas GMC provides good predictions of the effective moduli of short-fiber composites, it requires a simple modification when the inelastic behavior is sought. In addition, they provided an overview of the literature on this subject.

In a series of papers, Bednarcyk and Pindera [52–54] presented an extensive experimental and theoretical investigation of the behavior of woven carbon/copper composites. The modeling of the woven metal matrix composite was based on the two-dimensional doubly periodic MOC to represent the unidirectional infiltrated fiber yarn and embedded within the triply periodic GMC, which enabled representation of the composite's three-dimensional repeating unit cell. The reformulation of the GMC analysis of Pindera and Bednarcyk [12] has been employed to achieve computer time efficiency. In a more recent publication, Bednarcyk [55] presented a different modeling approach, based on the GMC, for woven polymer matrix composites. This approach is based on a two-step homogenization procedure in which the woven composite repeating unit cell is homogenized independently in the through-thickness direction prior to homogenization in the plane of the weave (see also [56] for a related discussion).

An evaluation of the performance of laminated metal matrix rotating shafts under various loading and damage conditions has been presented by Salzar [57]. This was accomplished through the development of an inelastic (classical plasticity and GVIPS constitutive laws) axisymmetric generalized plane-strain model that incorporates the GMC and includes the capability of fiber–matrix debond. In a subsequent paper [58], the influence of autofrettage on metal matrix composite-reinforced armaments has been studied by employing a multiply metal matrix layered cylinder in which the constitutive behavior of the unidirectional composite was modeled by the MOC.

In analyzing the effect of randomness in microstructural configuration on the material behavior of composites, the moving-window GMC technique has been used by Baxter and Graham [59], Baxter et al. [60], Graham and Baxer [61], and Siragy [62] to generate local fields of effective material properties associated with a given material microstructural image. The moving-window GMC technique is used to divide the heterogeneous image into small windows, and the GMC analysis is performed to homogenize these windows and produce a field of effective elastic properties at each of these windows. These fields are subsequently applied in finite element analyses, which are used to predict the local stresses associated with a given microstructure under prescribed loading and boundary conditions.

In a series of papers that considered elastic [63], elastoplastic [64], and viscoelastic [65] composites, the system of algebraic equations involved in the GMC analysis has been solved by utilizing a sparse solver. This enables a straightforward implementation of the GMC model with about 10,000 subcells. By using so many subcells, the authors were able to model complex microstructure architectures that require a high resolution.

Kumar and Singh [66] investigated the fiber arrangement effect on the creep behavior of a fiber-reinforced composite by using, in conjunction with the correspondence principle for viscoelastic material, the MOC, the cylindrical model, and the finite element method.

The micromechanically established constitutive equations by the GMC have been utilized to solve various composite structures. Examples are the analysis of postbuckling response of curved composite panels [67–71]; the analysis of metal matrix laminated tubes with internal fiber cracks [72]; the analysis of metal matrix plates subjected to nonuniform temperature loading [73]; the study of the dynamic response of metal matrix composite plates subjected to uniform temperature loading [74]; and parametric stability, buckling, and dynamic buckling of composite plates [75–77]. For a summary of recent investigations that address the analysis of bifurcation buckling, parametric stability, dynamic buckling, and thermally induced dynamic buckling of composite plates and shells in which the GMC has been used to determine the constitutive law of the composite, see [78].

The GMC was utilized in the analysis of thermal barrier coatings [79–81] and in the dynamic analysis of functionally graded materials [82].

The GMC approach has been also used by Fuchs et al. [83] for the topological design of structures by defining a domain of porous material, including the loads and supports, and finding an optimal distribution of densities. These authors showed that this approach is more efficient and less time consuming than the conventional method, where a series of preliminary finite element analyses of materials with different densities and aspect ratios has to be conducted followed by an interpolation technique to cover the density and aspect ration ranges.

The viscoelastic GMC approach, in which any one of the constituents can be considered to behave as a viscoelastic material, has been incorporated with a commerical structural analysis and optimization code referred to as HyperSizer [84]. HyperSizer is a unique state-of-the-art automated structural sizing software that currently performs strength and stability analyses of stiffened panels and beams when subjected to thermomechanical environments and provides analytical weight predictions (Collier Research Corp., 1998, http://collier-research.com/). Optimization capabilities include automatic selection from stiffened panel, sandwich panel, and beam concepts constructed of advanced composite, metallic, honeycomb, and foam materials.

Finally, Assaad and Arnold [85] employed the GMC through MAC software to analyze the tensile behavior of a nonlinear nylon-reinforced elastomeric composite system.

§3. THE GENERALIZED METHOD OF CELLS FOR SMART MULTIPHASE COMPOSITES

In this section, the GMC approach will be employed for prediction of the overall behavior of smart or intelligent composites, which consist of phases that can sense or actuate. These include electromagnetothermoelastic multiphase materials [86], of which piezoelectric composites [87] form a special case; electrostrictive composites [88] and shape-memory alloy composites [89].

3.1. *Electromagnetothermoelastic composites*

The constitutive equations that govern the interaction of elastic, electric, magnetic, and thermal fields in an electromagnetothermoelastic medium relate the stresses σ_{ij}, strains ϵ_{ij}, electric field E_i, magnetic field H_i, and temperature deviation ΔT from a reference temperature as follows:

$$\sigma_{ij} = C_{ijkl}\epsilon_{kl} - e_{kij}E_k - q_{kij}H_k - \Lambda_{ij}\Delta T \qquad i, j, k, l = 1, \ldots, 3 \tag{15}$$

where C_{ijkl}, e_{ijk}, q_{ijk}, and Λ_{ij} denote the fourth-order elastic stiffness tensor, the third-order piezoelectric tensor, the third-order piezomagnetic tensor, and the second-order thermal stress tensor of the material, respectively.

In addition, the electric displacement vector D_i is also expressed in terms of the strain, electric field, magnetic field, and temperature in the form

$$D_i = e_{ikl}\epsilon_{kl} + \kappa_{ik}E_k + a_{ik}H_k + p_i\Delta T \tag{16}$$

where κ_{ik}, a_{ik}, and p_i are the second-order dielectric tensor, the second-order magnetoelectric coefficient tensor, and the pyroelectric vector, respectively.

Finally, the magnetic flux density vector B_i is given in terms of the mechanical, electric, and magnetic fields and temperature by

$$B_i = q_{ikl}\epsilon_{kl} + a_{ik}E_k + \mu_{ik}H_k + m_i\Delta T \tag{17}$$

where μ_{ik} and m_i are the second-order magnetic permeability tensor and the pyromagnetic vector, respectively.

Let the vectors $\mathbf{X}$ and $\mathbf{Y}$ be defined as follows:

$$\mathbf{X} = [\epsilon_{11}, \epsilon_{22}, \epsilon_{33}, 2\epsilon_{23}, 2\epsilon_{13}, 2\epsilon_{12}, -E_1, -E_2, -E_3, -H_1, -H_2, -H_3] \tag{18}$$

$$\mathbf{Y} = [\sigma_{11}, \sigma_{22}, \sigma_{33}, \sigma_{23}, \sigma_{13}, \sigma_{12}, D_1, D_2, D_3, B_1, B_2, B_3] \tag{19}$$

Consequently, Eqs. (15)–(17) can be written in the following compact matrix form:

$$\mathbf{Y} = \mathbf{Z}\mathbf{X} - \mathbf{\Gamma}\Delta T \tag{20}$$

where the square 12th-order symmetric matrix of coefficients $\mathbf{Z}$ has the following form:

$$\mathbf{Z} = \begin{bmatrix} \mathbf{C} & \mathbf{e}^{\mathbf{t}} & \mathbf{q}^{\mathbf{t}} \\ \mathbf{e} & -\boldsymbol{\kappa} & -\boldsymbol{a} \\ \mathbf{q} & -\boldsymbol{a} & -\boldsymbol{\mu} \end{bmatrix} \tag{21}$$

and

$$\mathbf{\Gamma} = \begin{Bmatrix} \mathbf{\Lambda} \\ \mathbf{p} \\ \mathbf{m} \end{Bmatrix} \tag{22}$$

In Eq. (21), the square matrix $\mathbf{C}$ of the sixth order represents the fourth order stiffness tensor written in contracted notation, $\mathbf{e^t}$ denotes the transpose of the rectangular 3×6 matrix $\mathbf{e}$ that represents the corresponding third-order piezomagnetic tensor, $\mathbf{q^t}$ denotes the transpose of the rectangular 3×6 matrix $\mathbf{q}$ that represents the corresponding third-order piezomagnetic tensor, $\boldsymbol{\kappa}$ is a square matrix of the third order that corresponds to the dielectric tensor, $\mathbf{a}$ is a square matrix of the third order that represents the magnetoelectric coefficients, and $\boldsymbol{\mu}$ is a square matrix of the third order that represents the magnetic permeability tensor. Finally, the sixth-order vector $\mathbf{\Lambda}$ and the two third-order vectors, $\mathbf{p}$ and $\mathbf{m}$, in Eq. (22) represent the thermal stresses and pyroelectric and pyromagnetic coefficients, respectively.

In the framework of the GMC analysis, the volume average of the stresses $\bar{\sigma}_{ij}$, electric displacements $\bar{D}_i$, and the magnetic flux density $\bar{B}_i$ in the entire repeating cell (namely in the composite) is given by

$$\bar{\mathbf{Y}} = \frac{1}{DHL} \sum_{p=1}^{N_p} \sum_{q=1}^{N_q} \sum_{r=1}^{N_r} \sum_{\alpha,\beta,\gamma=1}^{2} d_\alpha^{(p)} h_\beta^{(q)} l_\gamma^{(r)} \mathbf{Y}^{(\alpha\beta\gamma)} \tag{23}$$

Similarly, the volume average of the strains $\bar{\epsilon}_{ij}$, electric field components $\bar{E}_i$, and magnetic field components $\bar{H}_i$ in the composite is given by

$$\bar{\mathbf{X}} = \frac{1}{DHL} \sum_{p=1}^{N_p} \sum_{q=1}^{N_q} \sum_{r=1}^{N_r} \sum_{\alpha,\beta,\gamma=1}^{2} d_\alpha^{(p)} h_\beta^{(q)} l_\gamma^{(r)} \mathbf{X}^{(\alpha\beta\gamma)} \tag{24}$$

With the linear expansions of the displacements and electric and magnetic potentials assumed by the GMC analysis, the static equilibrium and Maxwell's equations are satisfied. Hence, by applying the GMC analysis, which consists of imposing in the present electromagnetothermoelastic analysis the following interfacial conditions: (1) continuity of displacements, (2) continuity of tractions, (3) continuity of the electric potential, (4) continuity of normal electric displacements, (5) continuity of the magnetic potential, and (6) continuity of the normal magnetic flux density, one can establish the following localization relation between the local electromagnetoelastic field in the subcell $\mathbf{X}^{(\alpha\beta\gamma)}$ and the average external macrofield $\bar{\mathbf{X}}$ in the form [86]

$$\mathbf{X}^{(\alpha\beta\gamma)} = \mathbf{A}^{(\alpha\beta\gamma)} \bar{\mathbf{X}} \tag{25}$$

where $\mathbf{A}^{(\alpha\beta\gamma)}$ is the electromagnetoelastic concentration matrix associated with subcell $(\alpha\beta\gamma)$. Consequently, in conjunction with the averaging procedure given by Eq. (23), the following effective isothermal constitutive relations of the electromagnetoelastic composite can be established:

$$\bar{\mathbf{Y}} = \mathbf{Z}^* \bar{\mathbf{X}} \tag{26}$$

where the effective elastic stiffness, piezoelectric, piezomagnetic, dielectric, and magnetic permeability, and electromagnetic coefficients matrix $\mathbf{Z}^*$ of the composite are given

by

$$\mathbf{Z}^* = \frac{1}{DHL} \sum_{p=1}^{N_p} \sum_{q=1}^{N_q} \sum_{r=1}^{N_r} \sum_{\alpha,\beta,\gamma=1}^{2} d_\alpha^{(p)} h_\beta^{(q)} l_\gamma^{(r)} \mathbf{Z}^{(\alpha\beta\gamma)} \mathbf{A}^{(\alpha\beta\gamma)} \tag{27}$$

The structure of the square 12th-order symmetric matrix $\mathbf{Z}^*$ is of the form

$$\mathbf{Z}^* = \begin{bmatrix} \mathbf{C}^* & \mathbf{e}^{*\mathrm{t}} & \mathbf{q}^{*\mathrm{t}} \\ \mathbf{e}^* & -\boldsymbol{\kappa}^* & -\mathbf{a}^* \\ \mathbf{q}^* & -\mathbf{a}^* & -\boldsymbol{\mu}^* \end{bmatrix} \tag{28}$$

where $\mathbf{C}^*$, $\mathbf{e}^*$, $\mathbf{q}^*$, $\boldsymbol{\kappa}^*$, $\mathbf{a}^*$, and $\boldsymbol{\mu}^*$ are the effective elastic stiffness, piezoelectric, piezomagnetic, dielectric, and magnetic permeability, and electromagnetic coefficients, respectively.

To incorporate the thermal effects in the composite, we utilize Levin's result [10] to establish the effective thermal stress tensor Λ_{ij}^*, and pyroelectric and pyromagnetic coefficients, p_i^* and m_i^*. To this end let us define the following vector of thermal stresses, and pyroelectric and pyromagnetic coefficient material constants in the subcell $(\alpha\beta\gamma)$:

$$\boldsymbol{\Gamma}^{(\alpha\beta\gamma)} = [\Lambda_1, \Lambda_2, \Lambda_3, \Lambda_4, \Lambda_5, \Lambda_6, p_1, p_2, p_3, m_1, m_2, m_3]^{(\alpha\beta\gamma)} \tag{29}$$

The corresponding vector of effective values is defined by

$$\boldsymbol{\Gamma}^* = [\Lambda_1^*, \Lambda_2^*, \Lambda_3^*, \Lambda_4^*, \Lambda_5^*, \Lambda_6^*, p_1^*, p_2^*, p_3^*, m_1^*, m_2^*, m_3^*] \tag{30}$$

According to Levin's result, the relation between $\boldsymbol{\Gamma}^{(\alpha\beta\gamma)}$ and $\boldsymbol{\Gamma}^*$ can be expressed in terms of the electromagnetomechanical concentration matries $\mathbf{A}^{(\alpha\beta\gamma)}$ as given by Eq. (9). Thus, with the established electromagnetoelastic concentration matrix $\mathbf{A}^{(\alpha\beta\gamma)}$, Eq. (9) provides the effective thermal stress $\boldsymbol{\Lambda}^*$, pyroelectric vector $\mathbf{p}^*$, and pyromagnetic vector $\mathbf{m}^*$ of the composite.

Consequently, the final anisothermal micromechanically established constitutive law of the electromagnetothermoelastic multiphase composite is given by

$$\bar{\mathbf{Y}} = \mathbf{Z}^* \bar{\mathbf{X}} - \boldsymbol{\Gamma}^* \Delta T \tag{31}$$

The coefficients of thermal expansion, α_i, and the associated pyroelectric constants P_i and the pyromagnetic constants M_i of the monolithic material can be assembled to form the vector

$$\boldsymbol{\Omega} = [\alpha_1, \alpha_2, \alpha_3, \alpha_4, \alpha_5, \alpha_6, P_1, P_2, P_3, M_1, M_2, M_3]$$

This vector is given by

$$\boldsymbol{\Omega} = \mathbf{Z}^{-1} \boldsymbol{\Gamma} \tag{32}$$

where $\mathbf{Z}$ and $\boldsymbol{\Gamma}$ are given by Eqs. (21) and (22), respectively.

In the same manner, the effective coefficients of thermal expansion, α_i^*, and the associated pyroelectric constants P_i^* and the pyromagnetic constants M_i^* of the composite can be also assembled into the vector:

$$\boldsymbol{\Omega}^* = [\alpha_1^*, \alpha_2^*, \alpha_3^*, \alpha_4^*, \alpha_5^*, \alpha_6^*, P_1^*, P_2^*, P_3^*, M_1^*, M_2^*, M_3^*] \tag{33}$$

Once $\mathbf{Z}^*$ and $\mathbf{\Gamma}^*$ have been established according to Eqs. (28) and (30), this vector can be readily determined from

$$\mathbf{\Omega}^* = \mathbf{Z}^{*-1}\mathbf{\Gamma}^* \tag{34}$$

In a recent publication, Bednarcyk [90] extended the preceding micromechanical analysis to model thermoelectromagnetoelastic laminated composites of this type and to include possible inelastic deformation effects in the presence of a metallic matrix. The GMC analysis was also reformulated [90] to improve its computational efficiency.

3.2. *Electrostrictive composites*

Electrostriction is characterized by the mechanical deformation that occurs in a dielectric material when an electric field is applied. It occurs in any material but the strains generated in most dielectrics are too small to be utilized for sensing and actuating. Certain dielectrics (e.g., PMN ceramic), however, exhibit sufficiently large dielectric permittivities and there by generate appreciable polarization and strains that can be utilized in practical applications. Unlike piezoelectric materials, uncharged electrostrictives are isotropic and are not poled. In addition, the relationship between the induced strains and polarization in electrostrictive dielectrics is nonlinear of a second order.

Hom and Shankar [91] proposed a Helmholtz free energy function ψ, which is expressed in terms of the total strain ϵ_{ij}, polarization P_i, and temperature T. From this function the fully coupled constitutive equations of electrostrictive isotropic materials can be derived. This function is given by

$$\psi(\epsilon_{ij}, P_i, T) = \frac{C_{ijkl}}{2}\left[\epsilon_{ij} - \epsilon^{\mathrm{E}}_{ij} - \epsilon^{\mathrm{T}}_{ij}\right]\left[\epsilon_{kl} - \epsilon^{\mathrm{E}}_{kl} - \epsilon^{\mathrm{E}}_{kl}\right] + F(|\mathbf{P}|) \qquad i, j, k, l = 1, \ldots, 3 \tag{35}$$

where $\epsilon^{\mathrm{E}}_{ij}$ and $\epsilon^{\mathrm{T}}_{ij}$ are the electric and thermal strains, respectively; $C_{ijkl} = \lambda\delta_{ij}\delta_{kl} + \mu(\delta_{ik}\delta_{jl} + \delta_{il}\delta_{jk})$ are elastic stiffness coefficients of the material (λ and μ are the Lame constants of the isotropic material and δ_{ij} is the Kronecker delta); and $|\mathbf{P}| = \sqrt{P_1^2 + P_2^2 + P_3^2}$.

The components of the electric strain $\epsilon^{\mathrm{E}}_{ij}$ are given by

$$\epsilon^{\mathrm{E}}_{ij} = (Q_{11} - Q_{12})P_iP_j + Q_{12}P_kP_k\delta_{ij} \tag{36}$$

where Q_{11}, Q_{12} are the electrostrictive coefficients of the isotropic material, and $F(|\mathbf{P}|)$ is a function that reflects the symmetric quadratic dependence of the induced strain versus the electric field that is observed in electrostrictive materials and provides the saturation feature for high values of electric field. This function is given by Hom and Shankar [91] in the following form:

$$F(|\mathbf{P}|) = \frac{1}{2k_0}\left[|\mathbf{P}|\log\frac{|p_s + \mathbf{P}|}{|p_s - \mathbf{P}|} + p_s\log\left(1 - \frac{|\mathbf{P}|^2}{p_s^2}\right)\right] \tag{37}$$

where k_0 and p_s are two material constants.

The thermal strains ϵ^T_{ij} in Eq. (35) are given by

$$\epsilon^T_{ij} = \alpha(T - T_0)\delta_{ij} \tag{38}$$

where α is the coefficient of thermal expansion and T_0 is a reference temperature.

Once the Helmholtz function has been established, one can determine the stress σ_{ij} and electric field E_i components as follows:

$$\sigma_{ij} = \frac{\partial \psi}{\partial \epsilon_{ij}} \tag{39}$$

$$E_i = \frac{\partial \psi}{\partial P_i} \tag{40}$$

With ψ given by Eq. (35), the resulting constitutive relations of the electrostrictive material are given by

$$\sigma_{ij} = C_{ijkl}\left[\epsilon_{kl} - \epsilon_{kl}^{E} - \epsilon_{kl}^{T}\right] \tag{41}$$

$$E_i = -2(Q_{11} - Q_{12})\sigma_{ij}P_j - 2Q_{12}\sigma_{kk}P_i + f_i(|\mathbf{P}|) \tag{42}$$

where

$$f_i(|\mathbf{P}|) = \frac{\partial F}{\partial P_i} = \frac{1}{k_0}\frac{P_i}{|\mathbf{P}|}\tanh^{-1}\frac{|\mathbf{P}|}{p_s} \tag{43}$$

It should be noted that, in contrast to a piezoelectric material, Eq. (42) shows that an electrostrictive material that is not subjected to electric field will not polarize under mechanical loading.

Due to the nonlinearity of the constitutive equations, our analysis must be incremental. Furthermore, it is based on formulating the field equations in a tangential form. This formulation will provide systems of linear algebraic equations that need to be solved at each increment (which is of great advantage over solving nonlinear ones in a nontangential formulation).

To impose the equilibrium and Maxwell equations and the proper continuity conditions across the various interfaces of the composite, the constitutive relations of the electrostrictive ceramic material need to be given in terms of the increments of the mechanical stresses $\Delta\sigma_{ij}$ and electrical displacements ΔD_i as independent variables. The latter are given by

$$\Delta D_i = \epsilon_0 \Delta E_i + \Delta P_i \tag{44}$$

where ϵ_0 is the permittivity of free space.

After some lengthy manipulations, the tangential constitutive relation of the electrostrictive material can be represented in the following standard form:

$$\Delta\mathbf{Y} = \mathbf{Z}\Delta\mathbf{X} - \mathbf{\Gamma}\Delta T \tag{45}$$

where

$$\Delta\mathbf{X} = [\Delta\epsilon_{11}, \Delta\epsilon_{22}, \Delta\epsilon_{33}, 2\Delta\epsilon_{23}, 2\Delta\epsilon_{13}, 2\Delta\epsilon_{12}, -\Delta E_1, -\Delta E_2, -\Delta E_3] \tag{46}$$

$$\Delta\mathbf{Y} = [\Delta\sigma_{11}, \Delta\sigma_{22}, \Delta\sigma_{33}, \Delta\sigma_{23}, \Delta\sigma_{13}, \Delta\epsilon_{12}, \Delta D_1, \Delta D_2, \Delta D_3] \tag{47}$$

and ΔT is the temperature deviation from T_0. In Eq. (45), $\mathbf{Z}$ is the ninth-order symmetric tangent electromechanical matrix and $\mathbf{\Gamma}$ is the thermal stress-pyroelectric vector of the material.

In the framework of the linear expansions of the displacements and electric potential assumed by GMC analysis, the static equilibrium of the material within the subcell $(\alpha\beta\gamma)$ at any increment is satisfied, namely,

$$\partial_j \Delta\sigma_{ij}^{(\alpha\beta\gamma)} + \partial_j \Delta M_{ij}^{(\alpha\beta\gamma)} = 0 \tag{48}$$

where $M_{ij}^{(\alpha\beta\gamma)}$ is the Maxwell electrostatic stress tensor, which is defined as

$$M_{ij}^{(\alpha\beta\gamma)} = \epsilon_0 \left(E_i^{(\alpha\beta\gamma)} E_j^{(\alpha\beta\gamma)} - \frac{1}{2} E_k^{(\alpha\beta\gamma)} E_k^{(\alpha\beta\gamma)} \delta_{ij} \right)$$

Similarly, the Maxwell equation

$$\partial_i \Delta D_i^{(\alpha\beta\gamma)} = 0 \tag{49}$$

in the absence of volume charge density is satisfied.

It can be shown that the GMC micromechanical analysis establishes the following localization relation [88]:

$$\Delta\mathbf{X}^{(\alpha\beta\gamma)} = \mathbf{A}^{(\alpha\beta\gamma)} \Delta\bar{\mathbf{X}} + \mathbf{G}^{(\alpha\beta\gamma)} \Delta T \tag{50}$$

where $\mathbf{A}(\alpha\beta\gamma)$ and $\mathbf{G}^{(\alpha\beta\gamma)}$ denote the current electomechanical and thermal-pyroelectric concentration factors, respectively. Equation (50) expresses the average strain and electric field increments in the subcell $(\alpha\beta\gamma)$ in terms of the uniform overall strain and electric field increments (i.e., the applied macrostrain and macroelectric field increments) and temperature increment.

Substitution of Eq. (50) into Eq. (45) yields the following relation in the subcell:

$$\Delta\mathbf{Y}^{(\alpha\beta\gamma)} = \mathbf{Z}^{(\alpha\beta\gamma)} \left[\mathbf{A}^{(\alpha\beta\gamma)} \Delta\bar{\mathbf{X}} + \mathbf{G}^{(\alpha\beta\gamma)} \Delta T \right] - \mathbf{\Gamma}^{(\alpha\beta\gamma)} \Delta T \tag{51}$$

Consequently, in conjunction with the averaging procedure given by Eq. (23), the following effective tangential constitutive relations of the electrostrictive multiphase composite can be established:

$$\Delta\bar{\mathbf{Y}} = \mathbf{Z}^* \Delta\bar{\mathbf{X}} - \mathbf{\Gamma}^* \Delta T \tag{52}$$

where the current effective tangent tensor, which relates the average stress and electric displacement increments to the applied average strain and electric field increments, is given in a closed-form manner by Eq. (27), whereas the current effective thermal and pyroelectric vector is given by

$$\mathbf{\Gamma}^* = \frac{-1}{DHL} \sum_{p=1}^{N_p} \sum_{q=1}^{N_q} \sum_{r=1}^{N_r} \sum_{\alpha,\beta,\gamma=1}^{2} d_\alpha^{(p)} h_\beta^{(q)} l_\gamma^{(r)} \left[\mathbf{Z}^{(\alpha\beta\gamma)} \mathbf{G}^{(\alpha\beta\gamma)} - \mathbf{\Gamma}^{(\alpha\beta\gamma)} \right] \tag{53}$$

Finally, the effective thermal expansion and the associated pyroelectric coefficients of the composite are given by Eq. (34) with $\mathbf{Z}^*$ and $\mathbf{\Gamma}^*$ given earlier.

It should be noted that the structure of the ninth-order symmetric effective tangent matrix $\mathbf{Z}^*$ is identical to that of $\mathbf{Z}$ which describes the tangent matrix of the PMN ceramic.

It is interesting to note, as one might expect, that the derived macrosopic effective constitutive law, Eq. (52), has an identical form as the constitutive relation for the constituent electrostrictive material given in Eq. (45). This is due to the fact that one can construct the macroscopic instantaneous electromechanical tensors ($\mathbf{Z}^*$, $\mathbf{\Gamma}^*$) in terms of their respective local ones through the established evolving electromechanical and thermal-pyroelectric tensors ($\mathbf{Z}$, $\mathbf{\Gamma}$).

Once $\mathbf{Z}^*$ and $\mathbf{\Gamma}^*$ have been determined at the current stage of mechanical deformation and electric voltage, one can obtain the average current stress tensor $\bar{\boldsymbol{\sigma}}$ and the current electric displacement $\bar{\mathbf{D}}$ from the computed stresses and electrical displacements at the previous stage ($\bar{\boldsymbol{\sigma}}|_{\text{previous}}$, $\bar{\mathbf{D}}|_{\text{previous}}$ according to $\bar{\boldsymbol{\sigma}} = \bar{\boldsymbol{\sigma}}|_{\text{previous}} + \Delta\bar{\boldsymbol{\sigma}}$ and $\bar{\mathbf{D}} = \bar{\mathbf{D}}|_{\text{previous}} + \Delta\bar{\mathbf{D}}$. Slmilarly, the current local strains $\boldsymbol{\epsilon}^{(\alpha\beta\gamma)}$ and electric field $\mathbf{E}^{(\alpha\beta\gamma)}$ and average strains $\bar{\boldsymbol{\epsilon}}$ and electrical field $\bar{\mathbf{E}}$ can be determined in the same manner.

3.3. *Shape-memory alloy composites*

A uniaxial rate-independent constitutive law of the shape-memory alloy (SMA) fibers was originally given by Grasser and Cozzarelli [92]. This law was subsequently modified by Witting and Cozzarelli [93] to the form

$$\dot{\epsilon}_{11} = \frac{\dot{\sigma}_{11}}{E} + |\dot{\epsilon}_{11}| \left| \frac{\sigma_{11} - \beta_{11}}{\sigma_c} \right|^{n-1} \frac{\sigma_{11} - \beta_{11}}{\sigma_c} \tag{54}$$

$$\beta_{11} = E\alpha \left\{ \epsilon_{11} - \frac{\sigma_{11}}{E} + f_{\mathrm{T}} \operatorname{erf}\left[a\left(\epsilon_{11} - \frac{\sigma_{11}}{E} \right) \right] \right\} \tag{55}$$

where ϵ_{11}, σ_{11}, and β_{11} are the one-dimensional strain, stress, and back stess, respectively, and $\operatorname{erf}(x)$ denotes the error function. In these equations, the dot denotes the time derivative, E is the Young modulus, σ_c is a critical stess, n is a constant power controlling the sharpness of transition from elastic to inelastic region, f_{T} is a parameter that controls the type (twinning hysteresis or superelasticity) and amount of recovery during unloading, a is a constant controlling the smoothness of the curve near the origin, and α is a constant that determines the slope during inelastic deformation.

Let Y denote the value of the threshold stress required to start stress-induced phase transition. It can be shown [93] that the parameter σ_c can be expressed as follows:

$$\sigma_c = Y - f_{\mathrm{T}} E \alpha (1 + \alpha)^{1/n} \tag{56}$$

Witting and Cozzarelli [93] give a methodology that enables the determination of the model parameters from measured data. Furthermore, Lauermann [94] established the temperature dependence of these parameters for NiTi SMA from measurements. It turns out that the parameters a and n can be assumed to be temperature independent.

A multiaxial generalization of Eqs. (54) and (55) has been presented by Witting and Cozzarelli [93] and is given as follow:

$$\dot{\epsilon}_{ij} = \frac{1+\nu}{E}\dot{\sigma}_{ij} - \frac{\nu}{E}\dot{\sigma}_{kk}\delta_{ij} + \sqrt{3K_2}(3J_2)^{\frac{n-1}{2}} \frac{s_{ij} - b_{ij}}{\sigma_c} \tag{57}$$

$$b_{ij} = \frac{2}{3} E \alpha \epsilon^I_{ij} \left\{ 1 + f_{\mathrm{T}} \left(\frac{2}{3}\sqrt{3I_2} \right)^{-1} \operatorname{erf}\left(\frac{2a}{3}\sqrt{3I_2} \right) \right\} \tag{58}$$

where δ_{ij} is the Kronecker delta, and the inelastic strain (transformation strain) ϵ^I_{ij} denotes the difference between the total strain ϵ_{ij} and the elastic strain, namely, $\epsilon^I_{ij} = \epsilon_{ij} - (\frac{1+\nu}{E}\sigma_{ij} - \frac{\nu}{E}\sigma_{kk}\delta_{ij})$. In addition,

$$I_2 = \frac{1}{2}\epsilon^I_{ij}\epsilon^I_{ij}$$
$$J_2 = \frac{1}{2}\frac{s_{ij} - b_{ij}}{\sigma_c}\frac{s_{ij} - b_{ij}}{\sigma_c}$$
$$K_2 = \frac{1}{2}\dot{e}_{ij}\dot{e}_{ij}$$

where e_{ij}, s_{ij}, and b_{ij} are the deviatoric tensors of ϵ_{ij}, σ_{ij}, and β_{ij}, respectively. It can be easily verified that under uniaxial loading conditions these constitutive relations reduce to Eqs. (54) and (55) that describe the SMA one-dimensional behavior.

Grasser and Cozzarelli's [92] approach resembles the total deformation theory of plasticity. An incremental model for SMA which is similar to incremental inelasticity has been presented by Boyd and Lagoudas [95]. This SMA model has been incorporated by Goldstein [89] with the GMC analysis for the prediction of the response of SMA fibers embedded in metal matrix composites.

The constitutive model of Boyd and Lagoudas [95] for SMA fibers has been further extended by Lagoudas et al. [96] to include the effect of compressive loading and, therefore, allows cyclic loading. To this end, let A_{os}, A_{of}, M_{os}, M_{of} denote the austenitic start, austenitic finish, martensitic start, and martensitic finish temperatures under stress-free state, respectively. According to this model the phase transition fraction from austenitic to martensitic, $\xi = 0 \rightarrow 1$, is given by

$$\xi = 1 - \exp\left[a_M(M_{os} - T) + \frac{b_M}{H}\sigma_{ij}\Lambda_{ij}\right] \qquad M_f \leq T \leq M_s \tag{59}$$

whereas the phase transition fraction from martensitic to austenitic, $\xi = 1 \rightarrow 0$, is given by

$$\xi = \exp\left[a_A(A_{os} - T) + \frac{b_A}{H}\sigma_{ij}\Lambda_{ij}\right] \qquad A_s \leq T \leq A_f \tag{60}$$

where T is the temperature and H is a material constant. In addition,

$$M_s = M_{os} + \frac{1}{HC_M}\sigma_{ij}\Lambda_{ij} \qquad M_f = M_{of} + \frac{1}{HC_M}\sigma_{ij}\Lambda_{ij}$$
$$A_s = A_{os} + \frac{1}{HC_A}\sigma_{ij}\Lambda_{ij} \qquad A_f = A_{of} + \frac{1}{HC_A}\sigma_{ij}\Lambda_{ij}$$

where C_M, C_A are material constants, and $a_M = \ln(0.01)/(M_s - M_f)$, $a_A = \ln(0.01)/(A_s - A_f)$, $b_M = a_M/C_M$, $b_A = a_A/C_A$. Furthermore, the transformation strain rate $\dot{\epsilon}^{tr}_{ij}$ is given by

$$e^{\text{tr}}_{ij} = \Lambda_{ij}\dot{\xi} \tag{61}$$

with

$$\Lambda_{ij} = \begin{cases} \dfrac{3}{2} H \dfrac{s_{ij}}{\sigma_e} & \dot{\xi} > 0 \\ H \dfrac{\epsilon_{ij}^{tr}}{\epsilon_e^{tr}} & \dot{\xi} < 0 \end{cases} \tag{62}$$

where $\sigma_e = [(3/2)s_{ij}s_{ij}]^{1/2}$, $\epsilon_e^{\mathrm{tr}} = [(2/3)\epsilon_{ij}^{tr}\epsilon_{ij}^{tr}]^{1/2}$, and s_{ij} are the stress deviators. This SMA constitutive law has been recently included in GMC analysis by Gilat and Aboudi [97] for the prediction of the overall behavior of metal and polymer matrix composite plates with embedded SMA fibers.

Finally, the response of shape-memory fiber composities have been predicted by Kawai et al. [98] in conjunction with the MOC analysis. These authors used constitutive equations of the SMA fiber that describe the stress-induced rhombohedral and martensitic transformations under multiaxial stress conditions.

§4. The generalized method of cells with finite deformations

The GMC approach has been applied for the prediction of the response of multiphase composites in which any phase can behave as a finite thermoelastic [99, 100] or as a finite viscoelastic [101] material. The constituent response is determined from an internal energy function which for isotropic materials depends on the invariants of the deformation tensor and entropy. By determining the instantaneous concentration tensor from GMC analysis, one can proceed and establish the effective instantaneous stiffness tensor and the instantaneous thermal stress tensor and, thus, the resulting anisotropic nonlinear law of the multiphase material.

4.1. *Finite deformation of thermoelastic composites*

Consider a multiphase material with isotropic, thermoelastic, compressible material constituents. The internal energy per unit mass of the material for such a phase is given by

$$W = W(I_1, I_2, I_3, \eta) \tag{63}$$

where I_i are the invariants of the right Cauchy–Green deformation tensor $\mathbf{C}$ and η is the entropy per unit mass.

With $\mathbf{F}$ denoting the deformation gradient, $\mathbf{C}$ is given by

$$\mathbf{C} = \mathbf{F}^{\mathrm{t}}\mathbf{F} \tag{64}$$

where $\mathbf{F}^{\mathrm{t}}$ denotes the transpose of $\mathbf{F}$. The Cauchy–Green strain tensor $\mathbf{E}$ is given by

$$\mathbf{E} = \frac{1}{2}(\mathbf{C} - \mathbf{I}) \tag{65}$$

where $\mathbf{I}$ is the unit matrix.

The second (symmetric) Piola–Kirchhoff tensor $\mathbf{S}$ is given by

$$S_{ij} = 2\rho_0 \frac{\partial W}{\partial C_{ij}} \tag{66}$$

where ρ_0 is the initial density of the material. The temperature θ is given in terms of the entropy per unit mass η by

$$\theta = \frac{\partial W}{\partial \eta} \tag{67}$$

It is advantageous to represent the constitutive relations of the material in an incremental form, because the use of total field values in the micromechanical analysis leads to a system of nonlinear algebraic equations [102]. To this end, let us represent the constitutive law of the nonlinearly thermoelastic material in the following incremental form:

$$\Delta \mathbf{S} = \frac{1}{2}\mathbf{D}\Delta \mathbf{C} - \mathbf{\Gamma}\Delta\theta \tag{68}$$

where $\mathbf{D}$ and $\mathbf{\Gamma}$ denote the instantaneous mechanical and thermal tangent tensors, respectively. The tangent tensor $\mathbf{D}$ of the material at the current instant of loading is determined from

$$D_{ijkl} = 2\frac{\partial S_{ij}}{\partial C_{kl}} = 4\rho_0 \frac{\partial^2 W}{\partial C_{ij}\partial C_{kl}} \tag{69}$$

The current thermal tangent tensor $\mathbf{\Gamma}$ is determined from

$$\Gamma_{ij} = -\frac{\partial S_{ij}}{\partial \theta} = -2\rho_0 \frac{\partial^2 W}{\partial C_{ij}\partial \theta} \tag{70}$$

The actual stress is expressed by the first Piola–Kirchhoff tensor $\mathbf{T}$, which is related to $\mathbf{S}$ as follows:

$$\mathbf{T} = \mathbf{S}\mathbf{F}^{\mathrm{t}} \tag{71}$$

Consequently, in terms of $\mathbf{T}$ and $\mathbf{F}$ the incremental constitutive law of the material is

$$\Delta \mathbf{T} = \mathbf{R}\Delta \mathbf{F} - \mathbf{H}\Delta\theta \tag{72}$$

where

$$R_{ijkl} = Q_{ipkl}F_{jp} + S_{il}\delta_{jk} \tag{73}$$

with

$$Q_{ijkl} = D_{ijlp}F_{kp} \tag{74}$$

and

$$H_{ij} = \Gamma_{ik}F_{jk} \tag{75}$$

The GMC micromechanical analysis is based on the satisfaction of the equilibrium equations in the subcell, and the fulfillment of the continuity of displacement and tractions at the interfaces between the subcells in the repeating cells and between neighboring cells.

The resulting analysis establishes the instantaneous concentration tensor $\mathbf{A}^{(\alpha\beta\gamma)}$ and the instantaneous thermal tensor $\mathbf{G}^{(\alpha\beta\gamma)}$ in terms of which the localization relationship is [99].

$$\Delta\mathbf{F}^{(\alpha\beta\gamma)} = \mathbf{A}^{(\alpha\beta\gamma)}\Delta\bar{\mathbf{F}} + \mathbf{G}^{(\alpha\beta\gamma)}\Delta\theta \tag{76}$$

Equation (76) expresses the deformation gradient increment in the subcell $(\alpha\beta\gamma)$ in terms of the applied average (macro) deformation gradient and temperature increments, via the mechanical and thermal concentration tensors $\mathbf{A}^{(\alpha\beta\gamma)}$ and $\mathbf{G}^{(\alpha\beta\gamma)}$, respectively.

From the established tensors, the following overall (macroscopic) nonlinear thermoelastic constitutive law that governs the average behavior of the multiphase composite, which consists of nonlinearly thermoelastic phase, can be established:

$$\Delta\bar{\mathbf{T}} = \mathbf{R}^*\Delta\bar{\mathbf{F}} - \mathbf{H}^*\Delta\theta \tag{77}$$

where the current effective tangent tensor, which relates the average first Piola–Kirchhoff increment to the applied average deformation gradient increment, is given in a closed-form manner by

$$\mathbf{R}^* = \frac{1}{DHL}\sum_{p=1}^{N_p}\sum_{q=1}^{N_q}\sum_{r=1}^{N_r}\sum_{\alpha,\beta,\gamma=1}^{2} d_\alpha^{(p)} h_\beta^{(q)} l_\gamma^{(r)} \mathbf{R}^{(\alpha\beta\gamma)}\mathbf{A}^{(\alpha\beta\gamma)} \tag{78}$$

whereas the current effective thermal tensor is given by

$$\mathbf{H}^* = \frac{1}{DHL}\sum_{p=1}^{N_p}\sum_{q=1}^{N_q}\sum_{r=1}^{N_r}\sum_{\alpha,\beta,\gamma=1}^{2} d_\alpha^{(p)} h_\beta^{(q)} l_\gamma^{(r)} [\mathbf{R}^{(\alpha\beta\gamma)}\mathbf{G}^{(\alpha\beta\gamma)} - \mathbf{H}^{(\alpha\beta\gamma)}] \tag{79}$$

Once $\mathbf{R}^*$ and $\mathbf{H}^*$ have been determined at the current stage of deformation, one can obtain the current average stress tensor $\bar{\mathbf{T}}$ from the computed stress at the previous stage, $\bar{\mathbf{T}}|_{\text{previous}}$, according to $\bar{\mathbf{T}} = \bar{\mathbf{T}}|_{\text{previous}} + \Delta\bar{\mathbf{T}}$. The current local and average deformation gradients, $(\mathbf{F}^{(\alpha\beta\gamma)})$, and $\bar{\mathbf{F}}$, can be determined in the same manner.

The finite deformation analysis in conjunction with MOC of Aboudi [102] has been employed to predict the response of Blatz and Ko [103] material, which forms a porous rubberlike polymer with 47% porosity. The validity of the recently proposed nonlinearly elastic GMC prediction has been assessed by Aboudi and Arnold [99] by comparison with the response of porous materials obtained from the spherical model (whose prediction is valid for hydrostatic loading only), based on the analysis of Horgan [104]. This has been performed for three different types of nonlinearly compressible elastic materials, two of which are known as the harmonic material and the generalized Varga material. Good agreement between the two different models is shown in all three cases and for various amount of porosities. It should be emphasized that this validation is significant since although the spherical model is one-dimensional in spherical coordinates, it is fully three-dimensional when it is implemented in the framework of GMC geometry.

The aforementioned established constitutive law, Eq. (77), which describes the overall behavior of finite deformation of multiphase material, has been implemented by Aboudi and Arnold [99] to investigate their response under various types of loading under isothermal conditions. Several types of composites were considered, including continuous and discontinuous reinforced composites as well as cellular materials that consist of open and closed cells.

The anisothermal finite deformation response of rubberlike matrix composites has been investigated by Aboudi [100]. Special attention has been given to the thermoelastic inversion effect that is detected in rubber. Rubberlike materials exhibit a distinctive characteristic referred to as the thermoelastic invesion effect. In ordinary materials (e.g., metals and ceramics) that are subjected to prescribed extensions, the gradient of stress with respect to temperature is always negative. In rubberlike material, on the other hand, this gradient becomes positive at prescribed extensions beyond a critical level, thereafter increasing with extension. Similarly, in ordinary materials that are subjected to prescribed loadings, the gradient of deformation with respect to temperature is always positive. In rubberlike materials this gradient becomes negative for loadings beyond a critical value, thereafter decreasing with loading. Thus, beyond this critical value the rubber has a negative coefficient of thermal expansion. This anomalous behavior of rubberlike solids can be demonstrated by hanging a weight on a strip of rubber and changing the temperature. The weight will rise upwards when the rubber is heated and it will lower when it is cooled.

The behavior of the rubberlike matrix was described by the Helmboltz free energy function that was developed by Chadwick [105], Chadwick and Creasy [106], and Morman [107]. This free energy models the large thermoelastic deformation of the unreinforced matrix material and is able to capture the thermoelastic inversion effect. It is given by

$$\psi(\mathbf{C},\theta) = \frac{\kappa}{\rho_0}\left[g(J)\frac{\theta}{\theta_0} - \alpha_0 h(J)(\theta-\theta_0)\right] + \frac{\mu}{\rho_0}\left[f(\mathbf{C})\frac{\theta}{\theta_0} - \gamma l(\mathbf{C})\left(\frac{\theta}{\theta_0}-1\right)\right] + \psi_2(\theta) - \psi_2(\theta_0)\frac{\theta}{\theta_0} \tag{80}$$

where ψ_2 is a function of temperature; κ, μ, ρ_0, α_0, and θ_0 are the bulk modulus, shear modulus, material density in the undistorted configuration, initial volume coefficient of thermal expansion, and the reference temperature, respectively; and $\gamma(0 \leq \gamma \leq 1)$ is a nondimensional scalar. Furthermore, $f(\mathbf{C})$, $l(\mathbf{C})$, $g(J)$, and $h(J)$ are functions of the corresponding arguments with $J = \det \mathbf{F}$. The functions $g(J)$ and $h(J)$ are referred to as volumetric response functions, whereas $f(\mathbf{C})$, $l(\mathbf{C})$ are referred to as distorsional functions. These functions, which must satisfy certain normalization conditions, are given by Aboudi [100].

The Cauchy stress $\boldsymbol{\sigma}$ is obtained from the free energy function $\boldsymbol{\psi}$ by employing the relation

$$\boldsymbol{\sigma} = 2\rho\mathbf{F}\frac{\partial\psi}{\partial C}\mathbf{F}^{\mathrm{t}} \tag{81}$$

where ρ is the current mass density of the material ($\rho_0 = \rho J$). This yields

$$\boldsymbol{\sigma} = \frac{2\kappa}{J}\mathbf{F}\left[g'(J)\frac{\theta}{\theta_0} - \alpha_0 h'(J)(\theta-\theta_0)\right]\frac{\partial J}{\partial C}\mathbf{F}^{\mathrm{t}} + \frac{2\mu}{J}\mathbf{F}\left[f'(\mathbf{C})\frac{\theta}{\theta_0} - \gamma l'(\mathbf{C})\left(\frac{\theta}{\theta_0}-1\right)\right]\mathbf{F}^{\mathrm{t}} \tag{82}$$

By employing the identity $\partial J/\partial \mathbf{C} = J\mathbf{C}^{-1}/2$ we readily obtain the expression

$$\boldsymbol{\sigma} = \kappa\left[g'(J)\frac{\theta}{\theta_0} - \alpha_0 h'(J)(\theta-\theta_0)\right]\mathbf{I} + \frac{2\mu}{J}\mathbf{F}\left[f'(\mathbf{C})\frac{\theta}{\theta_0} - \gamma l'(\mathbf{C})\left(\frac{\theta}{\theta_0}-1\right)\right]\mathbf{F}^{\mathrm{t}} \tag{83}$$

where $\mathbf{I}$, as stated before, is the unit matrix.

The first Piola–Kirchhoff stress tensor $\mathbf{T}$ is given in terms of the Cauchy stress tensor $\boldsymbol{\sigma}$ by

$$\mathbf{T} = J\mathbf{F}^{-1}\boldsymbol{\sigma} \tag{84}$$

from which the tangential form of the nonlinear thermomechanical constitutive relation, which is given by Eq. (72), can be determined.

Applications of the finite deformation GMC micromechanical analysis have been given by Aboudi [100] for nylon/rubberlike matrix composites subjected to hydrostatic loading, thermal loading with prescribed extension, thermal loading with prescribed stress, free thermal expansion, and isothermal uniaxial loading. The occurrence of the thermoelastic inversion effect in the composite has been exhibited and discussed.

4.2. *Finite deformation of viscoelastic composites*

The GMC analysis has also been implemented to establish the finite constitutive law of a multiphase composite in which any phase is modeled as a nonlinear viscoelastic material [101]. The finite viscoelastic representation of the material is based on Simo's [108] generalization of the infinitesimal viscoelastic behavior to large strain. The energy functional is taken as

$$W\left(\mathbf{E}, \mathbf{H}^{(n)}\right) = W^{\infty}(\mathbf{E}) + \sum_{n=1}^{N} \mathbf{H}^{(n)}\mathbf{E} \tag{85}$$

where W^{∞} is the elastic strain energy for long-term deformations, $\mathbf{E}$ is the Cauchy–Green strain tensor, and $\mathbf{H}^{(n)}$ is a set of N internal variables. Using this energy representation in Eqs. (65) and (66), the following expression for the second Piola–Kirchhoff stress tensor is obtained:

$$\mathbf{S} = \frac{\partial W^{\infty}(\mathbf{E})}{\partial \mathbf{E}} + \sum_{n=1}^{N} \mathbf{H}^{(n)} \tag{86}$$

Because the long-term contribution can be related to the short-term one, it can be concluded that this model is based on the additive split of the stress tensor into initial and nonequilibrium parts.

Let the strain energy be expressed by the following series expansion:

$$W = W^{\infty} + \sum_{n=1}^{N} W^{(n)} \exp\left[-t/\lambda^{(n)}\right] \tag{87}$$

where $\lambda^{(n)}$ are relaxation times.

Motivated by the similarity of Eq. (86) and the equations of small strain viscoelasticity that correspond to the generalized Maxwell model, the internal variables $\mathbf{H}^{(n)}$ at time t can be expressed in terms of convolution integrals [108],

$$\mathbf{H}^{(n)}(t) = \int_0^t \dot{\mathbf{S}}^{(n)}(\tau) \exp\left[-(t-\tau)/\lambda^{(n)}\right] dr \tag{88}$$

where $\mathbf{S}^{(n)}$ are internal stresses obtained from the energy functions

$$\mathbf{S}^{(n)} = \frac{\partial W^{(n)}}{\partial \mathbf{E}} \tag{89}$$

and dot denotes a time derivative.

Next, the following simplification is introduced. It is assumed that in energy expansion (87) each term $W^{(n)}$ is just a scalar multiplier of $W^{(0)}$, namely $W^{(n)} = \delta^{(n)} W^{(0)}$, where $W^{(0)}$ is the short-term elastic energy function. The use of this assumption in Eq. (87) provides

$$W^{\infty} = W^{(0)} \left[1 - \sum_{n=1}^{N} \delta^{(n)} \right] \tag{90}$$

Consequently, the second Piola–Kirchhoff stress tensor can be readily determined from Eqs. (86) and (90) as

$$\mathbf{S}(t) = \mathbf{S}^{\infty}(t) + \sum_{n=1}^{N} \mathbf{H}^{(n)}(t) \tag{91}$$

where

$$\mathbf{S}^{\infty}(t) = \frac{\partial W^{\infty}}{\partial \mathbf{E}} = \left[1 - \sum_{n=1}^{N} \delta^{(n)} \right] \frac{\partial W^{(0)}}{\partial \mathbf{E}} \tag{92}$$

and

$$\mathbf{H}^{(n)}(t) = \int_0^t \delta^{(n)} \dot{\mathbf{S}}^{(0)}(\tau) \exp\left[-(t-\tau)/\lambda^{(n)} \right] d\tau \tag{93}$$

with $\mathbf{S}^{(0)} = \partial W^{(0)}/\partial \mathbf{E}$. As was indicated by Simo [108], the exponential terms in the kernels can be replaced by continuous spectrum or by fractional derivatives. Alternatively, these kernels can be replaced by power types of kernels.

Relations (91)–(93) form the constitutive law of a finite viscoelastic constituent, which is just one phase of the nonlinearly viscoelastic composite. The viscoelastic constituent is characterized by the proper choice of the short-term strain energy function $W^{(0)}$, the relaxation times $\lambda^{(n)}$, and the weighting factors $\delta^{(n)}$. It should be noted that finite elasticity is recovered for very slow and very fast processes.

The preceding constitutive relations cannot be used in the micromechanical formulation because they are not given in an incremental form. To cast these equations in incremental form, let us divide the total time interval into subintervals $[t_{m-1}, t_m]$ with a time step $\Delta t_m = t_m - t_{m-1}$. It can be shown [101] that the following incremental constitutive law that describes the finite deformation of the viscoelastic phase in terms of the first Piola–Kirchhoff can be established:

$$\Delta \mathbf{T} = \mathbf{V} \Delta \mathbf{F} - \mathbf{Y} \tag{94}$$

where

$$V_{ijrs} = \xi Q_{ikrs} F_{jk} + \eta \delta_{jr} S_{is}^{(0)} + \delta_{jr} \sum_{n=1}^{N} H_{is}^{(n)} \tag{95}$$

and

$$\mathbf{Y} = \sum_{n=1}^{N} \alpha^{(n)} \mathbf{H}^{(n)}(t_{m-1}) \mathbf{F}^{T} \tag{96}$$

In these equations $\xi = 1 - \Sigma_{n=1}^{N}(1-\beta^{(n)})\delta^{(n)}$, $\eta = 1 - \Sigma_{n=1}^{N}\delta^{(n)}$, $\alpha^{(n)} = 1 - \exp(-\Delta t_m/\lambda^{(n)})$, and $\beta^{(n)} = \alpha^{(n)}\lambda^{(n)}/\Delta t_m$, with

$$\mathbf{H}^{(n)}(t_m) = \exp\left[-\frac{\Delta t_m}{\lambda^{(n)}}\right]\mathbf{H}^{(n)}(t_{m-1}) + \delta^{(n)}\frac{\Delta \mathbf{S}^{(0)}}{\Delta t_m}\lambda^{(n)}\left[1 - \exp\left(\frac{\Delta t_m}{\lambda^{(n)}}\right)\right] \tag{97}$$

In the special case of a finite elastic material, $\delta^{(n)} = 0$, $\xi = \eta = 1$, and $\alpha^{(n)} = 0$, so that Eq. (74) reduces to the isothermal form of Eq. (72), with $\mathbf{V} = \mathbf{R}$.

With the incremental constitutive law of the single finite viscoelastic phase given by Eq. (94), one can proceed with the GMC nonlinear micromechnaical analysis to establish the localization relation [101]:

$$\Delta \mathbf{F}^{(\alpha\beta\gamma)} = \mathbf{A}^{(\alpha\beta\gamma)}\Delta \bar{\mathbf{F}} + \mathbf{A}^{V(\alpha\beta\gamma)}\mathbf{Y}_s \tag{98}$$

Equation (98) express the deformation gradient increment in the subcell $(\alpha\beta\gamma)$ in terms of the applied average (macro) deformation gradient increment $\Delta\bar{\mathbf{F}}$ via the current concentration tensor $\mathbf{A}^{(\alpha\beta\gamma)}$ and the history of deformation. The latter is accounted for via $\mathbf{Y}_s$, which involves the microscopic viscoelastic terms in all subcells. In Eq. (98), $\mathbf{A}^{V(\alpha\beta\gamma)}$ denotes the resulting viscoelastic concentration tensor that is operating on $\mathbf{Y}_s$. Both concentration tensors are given by closed-form complicated expressions that involve the geometric dimensions of the repeating volume element and the properties of materials that occupy the subcells.

As a result, the following overall (macroscopic) nonlinear viscoelastic constitutive law that governs the average behavior of the multiphase composite, which consists of nonlinearly viscoelastic phase, can be established:

$$\Delta \bar{\mathbf{T}} = \mathbf{V}^{*}\Delta \bar{\mathbf{F}} - \bar{\mathbf{Y}} \tag{99}$$

where the current effective tangent tensor, which relates the average first Piola–Kirchhoff increment to the applied average deformation gradient increment, is given in a closed-form manner by

$$\mathbf{V}^{*} = \frac{1}{DHL}\sum_{p=1}^{N_p}\sum_{q=1}^{N_q}\sum_{r=1}^{N_r}\sum_{\alpha,\beta,\gamma=1}^{2} d_{\alpha}^{(p)} h_{\beta}^{(q)} l_{\gamma}^{(r)} \mathbf{V}^{(\alpha\beta\gamma)} \mathrm{A}^{(\alpha\beta\gamma)} \tag{100}$$

The overall viscoelastic contribution that accounts for the history of deformation is given by

$$\bar{\mathbf{Y}} = \frac{1}{DHL}\sum_{p=1}^{N_p}\sum_{q=1}^{N_q}\sum_{r=1}^{N_r}\sum_{\alpha,\beta,\gamma=1}^{2} d_{\alpha}^{(p)} h_{\beta}^{(q)} l_{\gamma}^{(r)} \left[\mathbf{V}^{(\alpha\beta\gamma)}\mathbf{A}^{V(\alpha\beta\gamma)}\mathbf{Y}_s - \mathbf{Y}^{(\alpha\beta\gamma)}\right] \tag{101}$$

§5. THE HIGH-FIDELITY GENERALIZED METHOD OF CELLS

Despite the extensively demonstrated capability of the GMC to accurately predict the macroscopic response of multiphase materials with periodic microstructures, both in the elastic and inelastic regions, the method's accuracy of estimating local stress and strain fields is not as good as its macropredictive capability. This is rooted in the first-order representation of the displacement field in the individual phases and the manner of satisfying the traction and displacement continuity conditions between the phases. The net effect is the absence of so-called shear coupling, which ensures that both normal and shear stresses at the local level are present for a given macroscopically applied stress. As a result, local stress fields are not well captured by the GMC. Attempts to capture this effect have been presented by Williams and Aboudi [109], Gan et al. [110], Orozco and Gan [111], and Williams [112, 113] (who employed a fifth-order theory).

Most recently, a new micromechanics model has been developed to overcome the aforementioned shortcoming of GMC. The theoretical framework of this model was motivated by a higher-order theory that has been developed to analyze functionally graded materials [114] and utilizes the elements of the homogenization technique. This new model is referred to as HFGMC and is capable of accurate simulation of microlevel stress and strain fields and macrolevel constitutive response of multiphase materials subjected to multiaxial loading [115, 116]. Extensive comparison with analytical and numerical solutions for the response of unidirectional composites under axisymmetric, axial shear, and transverse loading has demonstrated the capability of the newly developed model to predict *both* the macroscopic response and the local field quantities with excellent accuracy. Furthermore, numerous comparisons of HFGMC results with the GMC prediction have been presented by Aboudi et al. [117]. In these investigations, the HFGMC model has been assumed to admit materials undergoing infinitesimal deformations, which are characterized by periodic microstructures in the plane perpendicular to the direction of continuous reinforcement. The individual phases may be modeled as transversely isotropic or orthotropic in the elastic domain, and isotropic in the inelastic domain, based on the classical incremental plasticity and unified viscoplasticity theories. The micromechanical analysis establishes a constitutive law that models the overall behavior of the multiphase thermo-inelastic material in the form of a relationship between the average stress and strain, overall inelastic strain, and thermal strain tensors, in conjunction with the effective elastic stiffness tensor. This micromechanically established overall constitutive equation can be used either in a standalone manner or as a subroutine in conjunction with a finite element package to analyze an appropriate composite structure.

The unifying framework for the model's construction is the homogenization technique, which provides the correct boundary conditions that must be applied to a repeating unit cell representing the material's periodic microstructure under multiaxial loading. The homogenization technique has been used by a number of investigators in conjunction with the finite element method to estimat the effective properties of periodic composites. It is based on a multiscale asymptotic expansion of the displacement field within a repeating unit cell. In the context of HFGMC, the homogenization technique was employed to construct a higher-order displacement field approximation at the local microstructural level of a multiphase periodic material in a consistent fashion and to derive the governing field equations and the boundary conditions that the displacement field must satisfy. However, the method of solution for the local displacement, strain, and stress fields within a repeating unit cell borrows concepts from the aforementioned theory for functionally graded materials, in contrast with the standard finite element analyses used in conjunction with the homogenization technique. Specifically, the solution is based on GMC-like volume discretization of the repeating unit cell of a periodic composite into parallelepiped generic cells which

are assigned material properties to mimic the material's periodic microstructure. The solution for the local displacement and stress fields within each generic cell of the repeating unit cell is generated by satisfying the field equations, in a volumetric sense, and traction and displacement continuity and periodic boundary conditions, in an average sense. The higher-order displacement field approximation at the generic cell level is similar to that employed in the theory for functionally graded materials with appropriate modifications that ensure periodicity of the material microstructure and the presence of macroscopically applied strains. The solution for the local stress and strain fields in each generic cell is ultimately expressed in terms of the macroscopically applied strains, thereby facilitating the construction of Hill's strain concentration tensors [118] employed in the calculation of the effective material properties. This is the same formulation as that employed in MAC/GMC, thereby facilitating incorporation of HFGMC into this user-friendly interface environment.

5.1. *Homogenization procedure*

Consider a multiphase composite in which the microstructures are distributed periodically in the space that is given with respect to the global coordinates (x_1, x_2, x_3) see Figure 1*a*. Figure 1*b* shows the repeating unit cell of the periodic composite. In the framework of the homogenization method the displacements are asymptotically expanded as follows:

$$u_i(\mathbf{x}, \mathbf{y}) = u_{0i}(\mathbf{x}, \mathbf{y}) + \delta u_{1i}(\mathbf{x}, \mathbf{y}) + \cdots \tag{102}$$

where $\mathbf{x} = (x_1, x_2, x_3)$ are the macroscopic (global) coordinates, and, $\mathbf{y} = (y_1, y_2, y_3)$ are the microscopic (local) coordinates that are defined with respect to the repeating unit cell. The size of the unit cell is further assumed to be much smaller than the size of the body so that the relation between the global and local systems is

$$y_i = \frac{x_i}{\delta} \tag{103}$$

where δ is a small scaling parameter characterizing the size of the unit cell. This implies that a movement of order unity on the local scale corresponds to a very small movement on the global scale.

The homogenization method is applied to composites with periodic microstructures. Thus,

$$u_{\alpha i}(\mathbf{x}, \mathbf{y}) = u_{\alpha i}(\mathbf{x}, \mathbf{y} + n_p \mathbf{d}_p) \tag{104}$$

with $\boldsymbol{\alpha} = 0, 1, \ldots,$ where n_p are arbitrary integer numbers and the constant vectors $\mathbf{d}_p$ determine the period of the structure.

Due to the change of coordinates from the global to the local systems the following relation must be employed in evaluating the derivative of a field quantity:

$$\frac{\partial}{\partial x_i} \rightarrow \frac{\partial}{\partial x_i} + \frac{1}{\delta} \frac{\partial}{\partial y_i} \tag{105}$$

The quantities u_{0i} are the displacements in the homogenized region and, hence, they are not functions of y_i.

Let

$$u_{0\mathrm{i}} = u_{0\mathrm{i}}(\mathbf{x}) \equiv \bar{u}_{\mathrm{i}} \tag{106}$$

and

$$u_{1i} \equiv \tilde{u}_i(\mathbf{x}, \mathbf{y}) \tag{107}$$

where the latter are the fluctuating displacements that are unknown periodic functions. These displacements arise due to the heterogeneity of the medium.

The strain components are determined from displacements expansion (102) yielding, in conjunction with Eq. (105), the following expression:

$$\epsilon_{ij} = \bar{\epsilon}_{ij}(\mathbf{x}) + \tilde{\epsilon}_{ij}(\mathbf{x}, \mathbf{y}) + O(\delta) \tag{108}$$

where

$$\bar{\epsilon}_{ij}(\mathbf{x}) = \frac{1}{2}\left(\frac{\partial \bar{u}_i}{\partial x_j} + \frac{\partial \bar{u}_j}{\partial x_i}\right) \tag{109}$$

and

$$\tilde{\epsilon}_{ij}(\mathbf{x}, \mathbf{y}) = \frac{1}{2}\left(\frac{\partial \tilde{u}_i}{\partial y_j} + \frac{\partial \tilde{u}_j}{\partial y_i}\right) \tag{110}$$

This shows that the strain components can be represented as a sum of the average strain $\bar{\epsilon}_{ij}(\mathbf{x})$ in the composite and a fluctuating $\tilde{\epsilon}_{ij}(\mathbf{x}, \mathbf{y})$. It can be easily shown that

$$\frac{1}{V_y}\int \epsilon_{ij} dV_y = \frac{1}{V_y}\int (\tilde{\epsilon}_{ij} + \bar{\epsilon}_{ij}) dV_y = \bar{\epsilon}_{ij}$$

where V_y is the volume of the repeating unit cell. This follows directly from the periodicity of the fluctuating strain, implying that the average of the fluctuating strain taken over the unit repeating cell vanishes. For a homogeneous material it is obvious that the fluctuating displacements and strains identically vanish.

Using Eq. (108), one can readily represent the displacements in the form

$$u_i(\mathbf{x}, \mathbf{y}) = \bar{\epsilon}_{ij} x_j + \tilde{u}_i + O(\delta^2) \tag{111}$$

For an elastic material the stresses are related to the strains according to Hooke's law as follows:

$$\sigma_{ij} = C_{ijkl}\, \epsilon_{kl} \tag{112}$$

where $C_{ijkl}(\mathbf{x})$ are the components of the stiffness tensor of the composite's phases. The stiffness tensor forms a periodic function that is defined in the unit repeating cell in terms of the local coordinates $\mathbf{y}$ such that

$$C_{ijkl}(\mathbf{x}) = C_{ijkl}(\mathbf{y}) \tag{113}$$

Substituting Eq. (108) into Eq. (112) and differentiating with respect to the microvariable coordinates y_i leads to

$$\frac{\partial}{\partial y_j}\{C_{ijkl}(\mathbf{y})\,[\bar{\epsilon}_{kl}(\mathbf{x}) + \tilde{\epsilon}_{kl}(\mathbf{x}, \mathbf{y})]\} = 0 \tag{114}$$

Let us define the following stress quantities:

$$\sigma^0_{ij} = C_{ijkl}(\mathbf{y})\,\bar{\epsilon}_{kl}(\mathbf{x}) \tag{115}$$

$$\sigma^1_{ij} = C_{ijkl}(\mathbf{y})\,\tilde{\epsilon}_{kl}(\mathbf{x},\mathbf{y}) \tag{116}$$

where the latter represents the fluctuating stresses.

It follows that

$$\frac{\partial \sigma^1_{ij}}{\partial y_j} + \frac{\partial \sigma^0_{ij}}{\partial y_j} = 0 \tag{117}$$

which are the strong forms of the equilibrium equations. It is readily seen that the first term in Eq. (117) involves the unknown fluctuating periodic displacements $\tilde{u}_i$, whereas the second term produces pseudobody forces whose derivatives are actually zero everywhere except at the interfaces between the phases.

For given values of the average strains $\bar{\epsilon}_{kl}$ the unknown fluctuating displacements are governed by Eqs. (117) subject to periodic boundary conditions that are prescribed at the boundaries of the repeating unit cell. In addition to these boundary conditions one needs to impose the continuity of displacements and tractions at the internal interfaces between the phases that fill the repeating unit cell.

Referring to Figure 1*b*, the repeating unit cell is given by a parallelepiped defined with respect to the local coordinates by $0 \le y_1 \le D$, $0 \le y_2 \le H$, and $0 \le y_3 \le L$. Consequently, the periodic boundary conditions are given by

$$\tilde{u}_i(y_1 = 0) = \tilde{u}_i(y_1 = D) \tag{118}$$

$$\sigma_{1i}(y_1 = 0) = \sigma_{1i}(y_1 = D) \tag{119}$$

$$\tilde{u}_i(y_2 = 0) = \tilde{u}_i(y_2 = H) \tag{120}$$

$$\sigma_{2i}(y_2 = 0) = \sigma_{2i}(y_2 = H) \tag{121}$$

$$\tilde{u}_i(y_3 = 0) = \tilde{u}_i(y_3 = L) \tag{122}$$

$$\sigma_{3i}(y_3 = 0) = \sigma_{3i}(y_3 = L) \tag{123}$$

where the total stress, which is given by Eq. (112), is expressed as

$$\sigma_{ij} = \sigma^0_{ij} + \sigma^1_{ij} \tag{124}$$

It is also necessary to fix the displacement field at a point in the repeating unit cell (e.g., at a corner).

Once a solution of Eqs. (117), subject to internal interfacial conditions and periodic boundary conditions (118)–(124), has been established, one can proceed and determine the strain concentrations tensor associated with the defined repeating unit cell. This tensor expresses the local strain in the cell in terms of the global applied external strain (localization). To this end let us define the fourth-order tensor $\tilde{\mathbf{A}}$ as follows:

$$\tilde{\boldsymbol{\epsilon}} = \tilde{\mathbf{A}}(\mathbf{y})\,\bar{\boldsymbol{\epsilon}} \tag{125}$$

It relates the fluctuating strain to the applied average strain. By using Eq. (108), we readily obtain the requested strain concentration tensor $\mathbf{A}(\mathbf{y})$ as follows:

$$\boldsymbol{\epsilon} = \bar{\boldsymbol{\epsilon}} + \tilde{\mathbf{A}}(\mathbf{y})\,\bar{\boldsymbol{\epsilon}} = [\mathbf{I}_4 + \tilde{\mathbf{A}}(\mathbf{y})]\bar{\boldsymbol{\epsilon}} \equiv \mathbf{A}(\mathbf{y})\bar{\boldsymbol{\epsilon}} \tag{126}$$

where $\mathbf{I}_4$ is the fourth order identity tensor.

To obtain the strain concentration tensor **A(y)** a series of problems must be solved as follows. Solve Eqs. (117) in conjunction with the internal interfacial and periodic boundary conditions with $\bar{\boldsymbol{\epsilon}}_{11} = 1$ and all other components being equal to zero. The solution of Eqs. (117) readily provides A_{ij11} for $i, j = 1, 2, 3$. This procedure is repeated with $\bar{\boldsymbol{\epsilon}}_{22} = 1$ and all other components equal to zero, which provides A_{ij22}, and so on.

Once the strain concentration tensor **A(y)** has been determined, it is possible to compute the effective stiffness tensor of the multiphase composite as follows. Substitution of $\boldsymbol{\epsilon}$ given by Eq. (126) in Eq. (112) yields

$$\boldsymbol{\sigma} = \mathbf{C}(\mathbf{y})\,\mathbf{A}(\mathbf{y})\bar{\boldsymbol{\epsilon}} \tag{127}$$

Taking the average of both sides of Eq. (127) over the repeating unit cell yields the average stress in the composite in terms of the average strain via the effective elastic stiffness tensor $\mathbf{C}^*$, namely,

$$\bar{\boldsymbol{\sigma}} = \mathbf{C}^*\bar{\boldsymbol{\epsilon}} \tag{128}$$

where

$$\mathbf{C}^* = \frac{1}{V_y}\int \mathbf{C}(\mathbf{y})\,\mathbf{A}(\mathbf{y})\,dV_y \tag{129}$$

5.2. *Method of solution*

The preceding analysis has been presented for a multiphase composite with elastic phases. HFGMC has been developed to analyze both thermoelastic [115] and thermoinelastic phases [116, 117]. To this end, an approximate solution for the displacement field is constructed based on volumetric averaging of the field equations together with the imposition of the periodic boundary conditions and continuity conditions in an average sense between the subcells used to characterize the materials' microstructure. This is accomplished by approximating the fluctuating displacement field in each subcell of the generic cell of Figure 1*c* using a quadratic expansion in terms of local coordinates $(\bar{y}_1^{(\alpha)}, \bar{y}_2^{(\beta)}, \bar{y}_3^{(\gamma)})$ centered at the subcell's midpoint. A higher-order representation of the fluctuating field is necessary to capture the local effects created by the field gradients and the microstructure of the composite. This is in sharp contrast with the GMC, where the displacement expansion is linear (see Eq. (3)).

The second-order expansion of the displacement vector $\mathbf{u}^{(\alpha\beta\gamma)}$ in the subcell is given in terms of the local coordinates of the subcell as follows:

$$\begin{aligned}\mathbf{u}^{(\alpha\beta\gamma)} = {} & \bar{\boldsymbol{\epsilon}}\mathbf{x} + \mathbf{W}_{(000)}^{(\alpha\beta\gamma)} + \bar{y}_1^{(\alpha)}\mathbf{W}_{(100)}^{(\alpha\beta\gamma)} + \bar{y}_2^{(\beta)}\mathbf{W}_{(010)}^{(\alpha\beta\gamma)} + \bar{y}_3^{(\gamma)}\mathbf{W}_{(001)}^{(\alpha\beta\gamma)} \\ & + \frac{1}{2}\left(3\bar{y}_1^{(\alpha)2} - \frac{d_\alpha^{(p)2}}{4}\right)\mathbf{W}_{(200)}^{(\alpha\beta\gamma)} + \frac{1}{2}\left(3\bar{y}_2^{(\beta)2} - \frac{h_\beta^{(q)2}}{4}\right)\mathbf{W}_{(020)}^{(\alpha\beta\gamma)} \\ & + \frac{1}{2}\left(3\bar{y}_3^{(\gamma)2} - \frac{l_\gamma^{(r)2}}{4}\right)\mathbf{W}_{(002)}^{(\alpha\beta\gamma)}\end{aligned} \tag{130}$$

where $\mathbf{W}_{(000)}^{(\alpha\beta\gamma)}$, which is the fluctuating volume-averaged displacement vector, and the higher-order terms $\mathbf{W}_{(lmn)}^{(\alpha\beta\gamma)}$ must be determined from coupled governing equations (117) as well as the periodic boundary conditions (118)–(123) that the fluctuating field must

fulfill, in conjunction with the interfacial continuity conditions between subcells. The total number of unknowns that describe the fluctuating field in the subcell $(\alpha\beta\gamma)$ is 21. Consequently, the governing equations for the interior and boundary cells form a system of $168N_pN_qN_r$ algebraic equations in the unknown field coefficients that appear in quadratic expansions (130).

The final form of this system of equations is symbolically represented by

$$\mathbf{KU} = \mathbf{f} + \mathbf{g} \tag{131}$$

where the structural stiffness matrix $\mathbf{K}$ contains information on the geometry and mechanical properties of the materials within the individual subcells $(\alpha\beta\gamma)$ within the cells comprising the multiphase periodic composite. The displacement vector $\mathbf{U}$ contains the unknown displacement coefficients in each subcell. The force $\mathbf{f}$ contains information on the thermomechanical properties of the materials filling the subcells, the applied average strains $\bar{\epsilon}_{ij}$, and the imposed temperature deviation ΔT. The inelastic force vector $\mathbf{g}$ appearing on the right-hand side of Eq. (131) contains the inelastic effects given in terms of the intergrals of the inelastic strain distributions. These integrals depend implicitly on the elements of the displacement coefficient vector $\mathbf{U}$, requiring an incremental procedure of Eq. (131) at each point along the loading path.

The solution of Eq. (131) enables the establishment of the following localization relation that expresses the average strain $\bar{\boldsymbol{\epsilon}}^{(\alpha\beta\gamma)}$ in the subcell $(\alpha\beta\gamma)$ to the external applied strain $\bar{\boldsymbol{\epsilon}}$ in the form [116, 117]

$$\bar{\boldsymbol{\epsilon}}^{(\alpha\beta\gamma)} = \mathbf{A}^{(\alpha\beta\gamma)}\bar{\boldsymbol{\epsilon}} + \mathbf{D}^{(\alpha\beta\gamma)} \tag{132}$$

where $\mathbf{A}^{(\alpha\beta\gamma)}$ is the mechanical strain concentration matrix of the subcell $(\alpha\beta\gamma)$, and $\mathbf{D}^{(\alpha\beta\gamma)}$ is a vector that involves the current thermo-inelastic effects in the subcell.

The final form of the effective constitutive law of the multiphase thermo-inelastic composite, which relates the average stress $\bar{\boldsymbol{\sigma}}$ and strain $\bar{\boldsymbol{\epsilon}}$, is established as follows:

$$\bar{\boldsymbol{\sigma}} = \mathbf{C}^*\bar{\boldsymbol{\epsilon}} - (\bar{\boldsymbol{\sigma}}^I + \bar{\boldsymbol{\sigma}}^T) \tag{133}$$

In this equation $\mathbf{C}^*$ is the effective elastic stiffness matrix of the composite whose form is identical to that given by Eq. (6), whereas the overall (macroscopic) thermal stresses in the composite are given by

$$\bar{\boldsymbol{\sigma}}^T = \boldsymbol{\Gamma}^*\Delta T \tag{134}$$

where $\boldsymbol{\Gamma}^*$ is given by Eq. (9). In should be emphasized that in employing Eq. (6) to determine $\mathbf{C}^*$ and Eq. (9) to determine $\boldsymbol{\Gamma}^*$ the concentration matrices $\mathbf{A}^{(\alpha\beta\gamma)}$, which have been established from the HFGMC analysis, have to be utilized. Finally, the overall (macroscopic) inelastic stresses in the composite are given by [116]

$$\bar{\boldsymbol{\sigma}}^I = \frac{-1}{DHL}\sum_{p=1}^{N_p}\sum_{q=1}^{N_q}\sum_{r=1}^{N_r}\sum_{\alpha,\beta,\gamma=1}^{2} d_\alpha^{(p)}h_\beta^{(q)}l_\gamma^{(r)}\left[\mathbf{C}^{(\alpha\beta\gamma)}\mathbf{D}^{(\alpha\beta\gamma)} - \mathbf{R}_{(0,0,0)}^{(\alpha\beta\gamma)} + (\mathbf{A}^{tr(\alpha\beta\gamma)} - \mathbf{I})\boldsymbol{\Gamma}^{(\alpha\beta\gamma)}\Delta T\right] \tag{135}$$

where the term $\mathbf{R}_{(0,0,0)}^{(\alpha\beta\gamma)}$ represents inelastic stress effects in the phase occupying the subcell $(\alpha\beta\gamma)$.

Alternatively, it is possible to establish $\mathbf{\Gamma}^*$ and $\bar{\boldsymbol{\sigma}}^I$ without utilizing Levin's result. This can be accomplished by representing $\bar{\boldsymbol{\epsilon}}^{(\alpha\beta\gamma)}$ in Eq. (132) in the form

$$\bar{\boldsymbol{\epsilon}}^{(\alpha\beta\gamma)} = \mathbf{A}^{(\alpha\beta\gamma)}\bar{\boldsymbol{\epsilon}} + \mathbf{A}^{th(\alpha\beta\gamma)}\Delta T + \mathbf{D}^{I(\alpha\beta\gamma)} \tag{136}$$

where the thermal concentration matrix $\mathbf{A}^{th(\alpha\beta\gamma)}$, which can be determined by applying a temperature deviation in the absence of mechanical loadings and inelastic effects, has been completely separated from the inelastic contribution $\mathbf{D}^{I(\alpha\beta\gamma)}$.

By using representation (136), the final form of the global constitutive relation is given again by Eq. (133), but with $\mathbf{\Gamma}^*$ expressed by

$$\mathbf{\Gamma}^* = \frac{-1}{DHL}\sum_{p=1}^{N_p}\sum_{q=1}^{N_q}\sum_{r=1}^{N_r}\sum_{\alpha,\beta,\gamma=1}^{2} d_\alpha^{(p)} h_\beta^{(q)} l_\gamma^{(r)}\left[\mathbf{C}^{(\alpha\beta\gamma)}\mathbf{A}^{th(\alpha\beta\gamma)} - \mathbf{\Gamma}^{(\alpha\beta\gamma)}\right] \tag{137}$$

and $\bar{\boldsymbol{\sigma}}^I$ given by

$$\bar{\boldsymbol{\sigma}}^I = \frac{-1}{DHL}\sum_{p=1}^{N_p}\sum_{q=1}^{N_q}\sum_{r=1}^{N_r}\sum_{\alpha,\beta,\gamma=1}^{2} d_\alpha^{(p)} h_\beta^{(q)} l_\gamma^{(r)}\left[\mathbf{C}^{(\alpha\beta\gamma)}\mathbf{D}^{I(\alpha\beta\gamma)} - \mathbf{R}_{(0,0,0)}^{(\alpha\beta\gamma)}\right] \tag{138}$$

5.3. *Applications*

As mentioned before, HFGMC has been applied to predict the macro- and microfields of thermoelastic [115] and thermo-inelastic composites [116, 117]. Furthermore, to illustrate the capabilities of HFGMC for simulating the response of composites with interfacial debonding, results from this new model have been compared with those obtained from the GMC [119]. Both micromechanics analyses employ a recently developed model [39] for the local fiber–matrix debonding that permits local stresses to unload after local debonding occurs.

The HFGMC has also been employed to predict the effective moduli of electromagnetothermoelastic composites [120]. Extensive comparisons with the predictions provided by the GMC and the results of Li and Dunn [121] (which are based on the Mori-Tanaka [122] model) exhibit excellent agreement.

The HFGMC has also been applied to investigate the finite deformation of multiphase materials in the presence of full thermomechanical coupling in the phase [123]. In this case the constitutive equations of the phase are derived from the free energy ψ given by Eq. (80) from which the stress tensor is obtained (see Eq. (81)). This free energy also provides the expression for the entropy by using the relation $\eta = -\partial\psi/\partial\theta$.

For the finite deformation of thermoelastic materials, the energy equation is given by

$$\rho_0\theta\frac{\partial\eta}{\partial t} - \operatorname{div}\mathbf{q} \tag{139}$$

This establishes the energy equation which can be shown [123] to take the nonlinear coupled heat equation form

$$\rho_0 c_v\dot{\theta} + \mathbf{B}\dot{\mathbf{F}} = -\operatorname{div}\mathbf{q} \tag{140}$$

where the components of the second-order tensor **B** are given by

$$B_{ik} = -\frac{\theta}{\theta_0}\left\{\kappa\left[\frac{\partial g}{\partial J} - \alpha_0\theta_0\frac{\partial h}{\partial J}\right]JC_{ij}^{-1} + 2\mu\left[\frac{\partial f}{\partial C_{ij}} - \gamma\frac{\partial l}{\partial C_{ij}}\right]\right\}F_{kj} \tag{141}$$

with C_{ij}^{-1} denoting the ij components of the inverse of **C**. The uncoupled heat equation is readily obtained from Eq. (140) by setting $\mathbf{B} = 0$ (yielding a one-way thermomechanical coupling). Finally, in the implementation of the energy equation, Eq. (140), the Fourier law, given by Eq. (14), is assumed to hold.

To demonstrate the predictive capability of HFGMC with continuously reinforced elastic composites undergoing finite deformations, comparisons with exact elasticity solutions [104] for a porous composite with four different types of matrix material under axisymmetric loading and a finite element analysis of a repeating unit cell representative of a unidirectionally reinforced periodic composite subjected to transverse loading have been reported by Aboudi and Pindera [124]. The comparisons of the predicted overall responses and internal fields with the exact and finite element solutions exhibit excellent agreement. Furthermore, examples of the nonlinear response of symmetric angle-ply laminates subjected to in-plane loading have been presented [124] in order to demonstrate the micromechanical model capability of predicting the behavior of this type of multidirectional reinforcements (such as biological tissues).

Extension of HFGMC to the analysis of thermoelastic-viscoplastic multiphase composites undergoing finite deformations has been recently presented by Aboudi [125]. To this end, the elastic-viscoplastic constitutive relations with isotropic and directional hardening by Rubin [126] (in which, in particular, the stress is not characterized by a hypoelastic equations so that no special rates of stress need to be considered) have been employed to model the finite deformations of the monolithic viscoplastic material.

REFERENCES

[1] J. Aboudi, *Mechanics of Composite Materials: A Unified Micromechanical Approach*, Elsevier, Amsterdam, 1991.

[2] S. Nemat-Nasser and M. Hori, *Micromechanics: Overall Properties of Heterogeneous Materials*, North-Holland, Amsterdam, 1999.

[3] J. Aboudi, Micromechanical Analysis of Composites by the Method of Cells—Update, *Appl. Mech. Rev.*, vol. 49, pp. S83–S91, 1996.

[4] B. A. Bednarcyk and S. M. Arnold, MAC/GMC 4. 0 User's Manual, NASA/TM-2002-212077, 2002.

[5] J. Aboudi, Generalized Effective Stiffness Theory for the Modeling of Fiber-Reinforced Composites, *Int. J. Solid Struct.*, vol. 17, pp. 1005–1018, 1981.

[6] J. Aboudi, A Continuum Theory for Fiber-Reinforced Elastic Viscoplastic Composites, *Int. J. Eng. Sci.*, vol. 20, pp. 605–621, 1982.

[7] M. Paley and J. Aboudi, Micromechanical Analysis of Composites by the Generalized Cells Model, *Mech. Mater.*, vol. 14, pp. 127–139, 1992.

[8] J. Aboudi, Micromechanical Analysis of Thermoinelastic Multiphase Short-Fiber Composites, *Compos. Eng.*, vol. 5, pp. 839–850, 1995.

[9] C. T. Herakovich, *Mechanics of Fibrous Composites*, Wiley, New York, 1998.

[10] V. M. Levin, On the Coefficients of Thermal Expansion of Heterogeneous Materials, *Mech. Solid*, vol. 2, pp. 58–61, 1967.

[11] G. J. Dvorak, Transformation Field Analysis of Inelastic Composite Materials, *Proc. R. Soc. Lond. A*, vol. 437, pp. 311–327, 1992.

[12] M.-J. Pindera and B. A. Bednarcyk, An Efficient Implementation of the Generalized Method of Cells for Unidirectional, Multi-Phased Composites with Complex Microstructures, *Compos. Part B—Eng.*, vol. 30, pp. 87–105, 1999.

[13] T. O. Williams and J. Aboudi, A Fully Coupled Thermomechanical Micromechanics Model, *J. Therm. Stresses*, vol. 22, pp. 841–873, 1999.
[14] D. H. Allen, Thermo-Mechanical Coupling in Inelastic Solids, *Appl. Mech. Rev.*, vol. 44, pp. 361–373, 1991.
[15] J. G. Bennett and K. S. Haberman, An Alternate Unified Approach to the Micromechanical Analysis of Composite Materials, *J. Compos. Mater.*, vol. 30, pp. 1732–1747, 1996.
[16] B. A. Bednarcyk and M.-J. Pindera, Inelastic Thermal Response of Gr/Cu with Nonuniform Fiber Distribution, *J. Aerospace Eng.*, vol. 9, pp. 93–105, 1996.
[17] A. D. Freed, K. P. Walker, and M. J. Verrilli, Extending the Theory of Creep to Viscoplasticity, *J. Press. Vess.*, vol. 116, pp. 67–75, 1996.
[18] T. O. Williams and M.-J. Pindera, An Analytical Model for the Inelastic Axial Shear Response of Unidirectional Metal Matrix Composites, *Int. J. Plasticity*, vol. 13, pp. 261–289, 1997.
[19] S. C. Baxter and M.-J. Pindera, Stress and Plastic Strain Fields During Unconstrained and Constrained Fabrication Cool Down of Fiber-Reinforced IMCs, *J. Compos. Mater.*, vol. 33, pp. 351–376, 1999.
[20] A. M. Roerden and C. T. Herakovich, The Inelastic Response of Porous, Hybrid-Fiber Composites, *Compos. Sci. Technol.*, vol. 60, pp. 2443–2454, 2000.
[21] P. C. Upadhyay and J. S. Lyons, Elastic Constants of Uniaxially Fiber Reinforced Multiphase Composites Using Recursive Cell Model, *J. Reinf. Plast. Compos.*, vol. 19. pp. 569–603, 2000.
[22] H. Mahiou and A. Béakou, Modelling of Interfacial Effects on the Mechanical Properties of Fibre-Reinforced Composites, *Compos. Part A—Appl. Sci.*, vol. 29, pp. 1035–1048, 1998.
[23] C. J. Lissenden, Fiber-Matrix Interfacial Constitutive Relations for Metal Matrix Composites, *Compos. Part B—Eng.*, vol. 30, pp. 267–278, 1999.
[24] A. Needleman, A Continuum Model for Void Nucleation by Inclusion Debonding. *J. Appl. Mech.*, vol. 54, pp. 525–531, 1987.
[25] C. J. Lissenden and S. M. Arnold, Theoretical and Experimental Considerations in Representing Macroscale Flow/Damage Surfaces for Metal Matrix Composites, *Int. J. Plasticity*, vol. 13, pp. 327–358, 1997.
[26] C. J. Lissenden and S. M. Arnold, Effect of Microstructural Architecture on Flow/Damage Surfaces for Metal Matrix Composites, in G. Z. Voyiadjis, J. L. Chaboche, and J. W. Ju (eds.), *Damage Mechanics in Engineering Materials*, pp. 385–400, Elsevier, Amsterdam 1998.
[27] S. K. Iyer, C. J. Lissenden, and S. M. Arnold, Local and Overall Flow in Composites Predicted by Micromechanics, *Compos. Part B—Eng.*, vol. 31, pp. 327–343, 2000.
[28] C. J. Lissenden, S. M. Arnold, and S. K. Iyer, Flow/Damage Surfaces for Fiber-Reinforced Metals Having Different Periodic Microstructures, *Int. J. Plasticity*, vol. 16, pp. 1049–1074, 2000.
[29] S. M. Arnold, A. F. Saleeb, and M. G. Castelli, A Fully Associative, Nonlinear Kinematic, Unified Viscoplastic Model for Titanium Based Matrices, *Life Prediction Methodology for Titanium Matrix Compsites*, pp. 231–256, ASTM-STP 1253, Philadelphia 1996.
[30] R. K. Goldberg and S. M. Arnold, A Study of Influencing Factors on the Tensile Response of a Titanium Matrix Composite with Weak Interfacial Bonding, NASA/TM-2000-209798, 2000.
[31] M. M. Aghdam, D. J. Smith, and M. J. Pavier, Finite Element Micromechanical Modelling of Yield and Collapse Behaviour of Metal Matrix Composites, *J. Mech. Phys. Solid*, vol. 48, pp. 499–528, 2000.
[32] N. K. Naik and V. K. Ganesh, Failure Behavior of Plain Weave Fabric Laminates Under Inplane Shear Loading, *J. Compos. Tech. Res.*, vol. 16, pp. 3–20, 1994.
[33] N. K. Naik and V. K. Ganesh, Failure Behavior of Plain Weave Fabric Laminates Under On-Axis Uniaxial Tensile Loading. 2. Analytical Predictions, *J. Compos. Mater.*, vol. 30, pp. 1779–1822, 1996.
[34] H. Mahiou and A. Béakou, Local Stress Concentration and the Prediction of Tensile Failure in Unidirectional Composites, *Compos. Sci. Technol.*, vol. 57, pp. 1661–1672, 1997.
[35] D. D. Robertson and S. Mall, Incorporating Fiber Damage in a Micromechanical Analysis of Metal Matrix Composite Laminates, *J. Compos. Tech. Res.*, vol. 18, pp. 265–273, 1996.

[36] W. A. Curtin, Theory of Mechanical Properties of Ceramic-Matrix Composites, *J. Am. Ceram. Soc.*, vol. 74, pp. 2837–2845, 1991.
[37] B. A. Bednarcyk and S. M. Arnold, Micromechanics-Based Deformation and Failure Prediction for Longitudinally Reinforced Titanium Composites, *Compos. Sci. Technol.*, vol. 61, pp. 705–729, 2001.
[38] W. A. Curtin, Ultimate Strengths of Fiber-Reinforced Ceramics and Metals, *Composites*, vol. 24, pp. 98–102, 1993.
[39] B. A. Bednarcyk and S. M. Arnold, Transverse Tensile and Creep Modeling of Continuously Reinforced Titanium Composites with Local Debonding, *Int. J. Solid Struct.*, vol. 39, pp. 1987–2017, 2002.
[40] M. A. Foringer, D. D. Robertson, and S. Mall, A Micromecanistic-Based Approach to Fatigue Life Modeling of Titanium-Matrix Composites, *Compos. Part B—Eng.*, vol. 28, pp. 507–521, 1997.
[41] S. R. Bodner, *Unified Plasticity for Engineering Applications*, Kluwer, New York, 2002.
[42] W. J. Fleming and A. L. Dowson, Prediction of the Fatigue Life of an Aluminium Metal Matrix Composite Using the Theory of Cells, *Sci. Eng. Compos.*, vol. 8, pp. 181–189, 1999.
[43] T. E. Wilt, S. M. Arnold, and A. F. Saleeb, A Coupled/Uncoupled Computational Scheme for Deformation and Fatigue Damage Analysis of Unidirectional Metal-Matrix Composites, pp. 65–82, ASTM STP 1315, Philadelphia 1997.
[44] S. M. Arnold and S. Kruch, Differential Continuum Damage Mechanics Models for Creep and Fatigue of Unidirectional Metal Matrix Composites, *Int. J. Damage Mech.*, vol. 3, pp. 170–191, 1994.
[45] B. A. Bednarcyk and S. M. Arnold, Fully Coupled Micro/Macro Deformation, Damage, and Failure Prediction for SiC/Ti-15-3 Laminates, *J. Aerospace Eng.*, vol. 15, pp. 74–83, 2002.
[46] G. Z. Voyiadjis and Z. Deliktas, Damage in MMCs Using the GMC: Theoretical Formulation, *Compos. Part B—Eng.*, vol. 28, pp. 597–611, 1997.
[47] G. Z. Voyiadjis and Z. Guelzim, A Coupled Incremental Damage and Plasticity Theory for Metal Matrix Composites, *J. Mech. Beh. Mater.*, vol. 6, pp. 193–219, 1996.
[48] G. Z. Voyiadjis and P. I. Kattan, *Advances in Damage Mechanics: Metal and Metal Matrix Composites*, Elsevier, Amsterdam, 1999.
[49] A. P. Raynolds and S. C. Baxter, Kinematic Hardening in a Dispersion Strengthened Aluminum Alloy: Experiment and Modeling, *Mater. Sci. Tech.*, vol. A285, pp. 265–279, 2000.
[50] C. T. Herakovich and S. C. Baxter, Influence of Pore Geometry on the Effective Response of Porous Media, *J. Mater. Sci.*, vol. 34, pp. 1595–1609, 1999.
[51] D. H. Pahr and S. M. Arnold, The Applicability of the Generalized Method of Cells for Analyzing Discontinuously Reinforced Composites, *Compos. Part B—Eng.*, vol. 33, pp. 153–170, 2002.
[52] B. A. Bednarcyk and M.-J. Pindera, Inelastic Response of a Woven Carbon/Copper Composite Part I: Experimental Characterization, *J. Compos. Mater.*, vol. 33, pp. 1807–1836, 1999.
[53] B. A. Bednarcyk and M.-J. Pindera, Inelastic Response of a Woven Carbon/Copper Composite Part II: Micromechanics Model, *J. Compos. Mater.*, vol. 34, pp. 299–331, 2000.
[54] B. A. Bednarcyk and M.-J. Pindera, Inelastic Response of a Woven Carbon/Copper Composite Part III: Model-Experiment Correlation, *J. Compos. Mater.*, vol. 34, pp. 352–378, 2000.
[55] B. A. Bednarcyk, Modeling Woven Polymer Matrix Composites with MAC/GMC, NASA/CR-2000-210370, 2000. See also: B. A. Bednarcyk and S. M. Arnold, Micromechanics-Based Modeling Woven Polymer Matrix Composites, *AIAA J.*, vol. 41, pp. 1788–1796, 2003.
[56] B. A. Bednarcyk, Discussion of "Woven Fabric Composite Material Model with Material Non-Linearity for Non-Linear Finite Element Simulation" by Tabiei and Jiang, *Int. J. Solid Struct.*, vol. 38, pp. 8585–8588, 2001.
[57] R. S. Salzar, Influence of Autofrettage on Metal Matrix Composite Reinforced Armaments, *Compos. Part B—Eng.*, vol. 30, pp. 841–847, 1999.

[58] R. S. Salzar, Design Considerations for Rotating Laminated Metal Matrix Composite Shafts, *Compos. Sci. Technol.*, vol. 59, pp. 883–897, 1999.

[59] S. C. Baxter and L. L. Graham, Characterization of Random Composites Using Moving-Window Technique, *J. Eng. Mech.*, vol. 126, pp. 389–397, 2000.

[60] S. C. Baxter, M. I. Hossain, and L. L. Graham, Micromechanics Based Random Material Property Fields for Particulate Reinforced Composites, *Int. J. Solid Struct.*, vol. 38, pp. 9209–9220, 2001.

[61] L. L. Graham and S. C. Baxter, Simulation of Local Material Properties Based on Moving-Window GMC, *Probabilist. Eng. Mech.*, vol. 16, pp. 295–305, Charlottesville 2001.

[62] E. Siragy, Characterization of Local Response of Heterogeneous Materials Using Moving-Window GMC and Finite Element Analysis, Ph. D. dissertation, University of Virginia, 2002. See also: L. L. Graham–Brady, E. F. Siragy, and S. C. Baxter, Analysis of Heterogeneous Composites Based on Moving–Window Techniques, *J. Eng. Mech*., vol. 129, pp. 1054–1064, 2003.

[63] C. E. Orozco, Computational Aspects of Modeling Complex Microstructure Composites Using GMC, *Compos. Part B—Eng.*, vol. 28, pp. 167–175, 1997.

[64] C. E. Orozco and M.-J. Pindera, Plastic Analysic of Complex Microstructure Composites Using the Generalized Method of Cells, *AIAA J.*, vol. 37, pp. 482–488, 1999.

[65] C. E. Orozco and M.-J. Pindera, Viscoelastic Analysis of Multi-Phase Composites Using the Generalized Method of Cells, *AIAA J.*, vol. 40, pp. 1619–1626, 2002.

[66] S. Kumar and R. N. Singh, The Creep Response of Uni-Directional Fiber-Reinforced Ceramic Composites: A Theoretical Study, *Compos. Sci. Technol.*, vol. 61, pp. 461–473, 2001.

[67] A. K. Noor, J. H. Starnes, and J. M. Peters, Nonlinear and Postbuckling Responses of Curved Composite Panels with Cutouts, *Compos. Struct.*, vol. 34, pp. 213–240, 1996.

[68] A. K. Noor and J. M. Peters, Nonlinear and Postbuckling Analyses of Curved Composite Panels Subjected to Combined Temperature Change and Edge Shear, *Comput. Struct.*, vol. 60, pp. 853–874, 1996.

[69] A. K. Noor and Y. H. Kim, Buckling and Postbuckling of Composite Panels with Cutouts Subjected to Combined Edge Shear and Temperature Change, *Comput. Struct.*, vol. 60, pp. 203–222, 1996.

[70] A. K. Noor and Y. H. Kim, Buckling and Postbuckling of Composite Panels with Cutouts Subjected to Combined Loads, *Finite Elem. Anal. Des.*, vol. 22, pp. 163–185, 1996.

[71] A. K. Noor, Recent Advances in Sensitivity Analysis for Thermomechanical Postbuckling of Composite Panels, *J. Eng. Mech.*, vol. 122, pp. 300–307, 1996.

[72] S. C. Baxter and M.-J. Pindera, Degradation of Elastic Response of MMC Laminated Tubes due to Internal Fiber Cracks, *J. Aerospace Eng.*, vol. 10, pp. 43–48, 1997.

[73] E. Feldman and I. Belostotsky, On the Response of MMC Laminated Plates to Non-Uniform Temperature Loading: The Effect of Temperature-Dependent Material Properties, *Compos. Struct.*, vol. 38, pp. 83–89, 1997.

[74] E. Feldman and R. Gilat, On the Dynamic Response of Metal Matrix Composite Panels to Uniform Temperature Loading, *Compos. Struct.*, vol. 47, pp. 619–624, 1999.

[75] R. Gilat and J. Aboudi, Parametric Stability of Non-Linearly Elastic Composite Plates by Lyapunov Exponents, *J. Sound Vib.*, vol. 235, pp. 727–637, 2000.

[76] R. Gilat, T. O. Williams, and J. Aboudi, Buckling of Composite Plates by Global-Local Theory, *Compos. Part B—Eng.*, vol. 32, pp. 229–236, 2001.

[77] R. Gilat and J. Aboudi, The Lyapunov Exponents as a Quantitative Criterion for the Dynamic Buckling of Composite Plates, *Int. J. Solid Struct.*, vol. 39, pp. 467–481, 2002.

[78] R. Gilat and J. Aboudi, Buckling Analysis of Composite Plates, in D. Durban, D. Givoli, and J. G. Simmonds (eds.), *Advances in the Mechanics of Plates and Shells*, pp. 135–150, Kluwer, Dordrecht 2001.

[79] M.-J. Pindera, J. Aboudi, and S. M. Arnold, Thermomechanical Analysis of Functionally Graded Thermal Barrier Coatings with Different Microstructural Scales, *J. Am. Ceram. Soc.*, vol. 81, pp. 1525–1536, 1998.

[80] M.-J. Pindera, J. Aboudi, and S. M. Arnold, The Effect of Interface Roughness and Oxide Film Thickness on the Inelastic Response of Thermal Barrier Coatings to Thermal Cycling, *J. Mater. Sci. Eng. A*, vol. 284, pp. 158–175, 2000.

[81] M.-J. Pindera, J. Aboudi, and S. M. Arnold, Analysis of Spallation Mechanism in Thermal Barrier Coatings with Graded Bond Coats Using the Higher-Order Theory for FGM's, *Eng. Fract. Mech.*, vol. 69, pp. 1587–1606, 2002.

[82] L. Banks-Sills, R. Eliasi, and Y. Berlin, Modeling of Functionally Graded Materials in Dynamic Analyses, *Compos. Part B—Eng.*, vol. 33, pp. 7–15, 2002.

[83] M. B. Fuchs, M. Paley, and E. Miroshny, The Aboudi Micromechanical Model for Topology Design of Structures, *Comput. Struct.*, vol. 73, pp. 355–362, 1999.

[84] C. S. Collier, HITEMP Material and Structural Optimization Technology Transfer, NASA CR-2001-211166, 2001.

[85] M. Assaad and S. M. Arnold, An Analysis of the Macroscopic Tensile Behavior of a Nonlinear Nylon Reinforced Elastomeric Composite System Using MAC/GMC, NASA/TM-1999-209066, 1999.

[86] J. Aboudi, Micromechanical Prediction of the Effective Behavior of Fully Coupled Electro-Magneto-Thermo-Elastic Multiphase Composites, NASA/CR-2000-209787, 2000.

[87] J. Aboudi, Micromechanical Prediction of the Effective Coefficients of Thermo-Piezoelectric Multiphase Composites, *J. Intel. Mater. Syst. Struct.*, vol. 9, pp. 713–722, 1998.

[88] J. Aboudi, Micromechanical Prediction of the Response of Electrostrictive Multiphase Composites, *Smart Mater. Struct.*, vol. 8, pp. 663–671, 1999.

[89] A. Goldstein, The Prediction of the Behavior of Composite Materials with Embedded SMA Fibers, M. Sc. thesis, Tel Aviv University, Tel Aviv, Israel, 2000.

[90] B. A. Bednarcyk, An Inelastic Micro/Macro Theory for Hybrid Smart/Metal Composites, *Compos. Part B—Eng.*, vol. 34, pp. 175–197, 2003.

[91] C. L. Hom and N. Shankar, A Fully Coupled Constitutive Model for Electrostrictive Ceramic Materials, *J. Intel. Mater. Syst. Struct.*, vol. 5, pp. 795–801, 1994.

[92] E. J. Graesser and F. A. Cozzarelli, A Proposed Three-Dimensional Constitutive Model for Shape Memory Alloys, *J. Intel. Mater. Syst. Struct.*, vol. 5, pp. 78–89, 1994.

[93] P. R. Witting and F. A. Cozzarelli, Experimental Determination of Shape Memory Alloy Constitutive Model Parameters, Active Materials and Smart Structures, *SPIE—Int. Soc. Opt. Eng.*, vol. 2477, pp. 260–275, 1995.

[94] M. E. Lauermann, Temperature Dependence of Shape Memory Material Parameters in Constitutive Law for Nitinol, M. Sc. thesis, State University of New York at Buffalo, New York, 1994.

[95] J. G. Boyd and D. C. Lagoudas, Thermomechanical Response of Shape Memory Composites, *J. Intel. Mater. Syst. Struct.*, vol. 5, pp. 333–346, 1994.

[96] D. C. Lagoudas, Z. Bo, and M. A. Qidwai, A Unified Thermodynamic Constitutive Model for SMA and Finite Element Analysis of Active Metal Matrix Composites, *Mech. Compos. Mater. Struct.*, vol. 3, pp. 153–179, 1996.

[97] R. Gilat and J. Aboudi, Dynamic Response of Active Composite Plates: Shape Memory Alloy Fibers in Polymeric/Metallic Matrices, *Int. J. Solid Structure*, 2004.

[98] M. Kawai, H. Ogawa, V. Baburaj, and T. Koga, Micromechanical Analysis for Hysteretic Behavior of Unidirectional TiNi SMA Fiber Composites, *J. Intel. Mater. Syst. Struct.*, vol. 10, pp. 14–28, 1999.

[99] J. Aboudi and S. M. Arnold, Micromechanical Modeling of the Finite Deformation of Thermoelastic Multiphase Composites, *Math. Mech. Solid*, vol. 5, pp. 75-99, 2000.

[100] J. Aboudi, Micromechanical Prediction of the Finite Thermoelastic Response of Rubberlike Matrix Composites, *J. Appl. Math. Phys. (ZAMP)*, vol. 52, pp. 823–846, 2001.

[101] J. Aboudi, Micromechanical Modeling of Finite Viscoelastic Multiphase Composites, *J. Appl. Math. Phys. (ZAMP)*, vol. 51, pp. 114–134, 2000.

[102] J. Aboudi, Overall Finite Deformation of Elastic and Elastoplastic Composites, *Mech. Mater.*, vol. 5, pp. 73–86, 1986.

[103] P. J. Blatz and W. L. Ko, Application of Finite Elastic Theory to the Deformation of Rubbery Materials, *Trans. Soc. Rheol.*, vol. 6, pp. 223–251, 1962.
[104] C. O. Horgan, On Axisymmetric Solutions for Compressible Nonlinearly Elastic Solids, *J. Appl. Math. Phys. (ZAMP)*, vol. 46, pp. S107–S125, 1995.
[105] P. Chadwick, Thermo-Mechanics of Rubberlike Materials, *Philos. Trans. R. Soc. A.*, vol. A276, pp. 372–403, 1974.
[106] P. Chadwick and C. F. M. Creasy, Modified Entropic Elasticity of Rubberlike Material, *J. Mech. Phys. Solid*, vol. 32, pp. 337–357, 1984.
[107] K. N. Morman, A. Thermomechanical Model for Amorphous Polymers in the Glassy, Transition, and Rubber Regions, AMD vol. 203, *Current Research in the Thermo-Mechanics of Polymers in the Rubbery-Glassy Range*, ASME, New York 1995.
[108] J. C. Simo, On a Fully Three-Dimensional Finite-Strain Viscoelastic Damage Model: Reforulation and Computational Aspects, *Comput. Method Appl. Mech.*, vol. 60, pp. 153–173, 1987.
[109] T. O. Williams and J. Aboudi, A Generalized Micromechanics Model with Shear-Coupling, *Acta Mech.*, vol. 138, pp. 131–154, 1999.
[110] H. Gan, C. E. Orozco, and C. T. Herakovich, A Strain-Compatible Method for Micromechanical Analysis of Multi-Phase Composites, *Int. J. Solid Struct.*, vol. 37, pp. 5097–5122, 2000.
[111] C. E. Orozco and H. Gan, Viscoplastic Response of Multiphase Composites Using a Strain-Compatible Volume-Averaging Method, *Compos. Part B—Eng.*, vol. 33, pp. 301–313, 2002.
[112] T. O. Williams, A Two-Dimensional, Higher-Order, Elasticity-Based Micromechanics Model, *Compos. Sci. Technol.*, to appear.
[113] T. O. Williams, A. Three-Dimensional, Higher-Order, Elasticity-Based Micromechanics Model, *Compos. Sci. Technol.*, to appear.
[114] J. Aboudi, M.-J. Pindera, and S. M. Arnold, Higher-Order Theory for Functionally Graded Materials, *Compos. Part B—Eng.*, 30, pp. 777–832, 1999.
[115] J. Aboudi, M.-J. Pindera, and S. M. Arnold, Linear Thermoelastic Higher-Order Theory for Periodic Multiphase Materials, *J. Appl. Mech.*, vol. 68, pp. 697–707, 2001.
[116] J. Aboudi, M.-J. Pindera, and S. M. Arnold, Higher-Order Theory for Periodic Multiphase Materials with Inelastic Phases, *Int. J. Plasticity*, vol. 19, pp. 805–847, 2003.
[117] J. Aboudi, M.-J. Pindera, and S. M. Arnold, High-Fidelity Generalized Method of Cells for Inelastic Periodic Multiphase Materials, NASA TM-2002-211469, 2002.
[118] R. Hill, Elastic Properties of Reinforced Solids: Some Theoretical Principles, *J. Mech. Phys. Solid*, vol. 11, pp. 357–372, 1963.
[119] B. A. Bednarcyk, S. M. Arnold, J. Aboudi, and M.-J. Pindera, Local Field Effects in Titanium Matrix Composites Subjected to Fiber-Matrix Debondig, *Int. J. Plasticity*, 2004.
[120] J. Aboudi, Micromechanical Analysis of Fully Coupled Electro-Magneto-Thermo-Elastic Multiphase Composites, *Smart Mater. Struct.*, vol. 10, pp. 867–877, 2001.
[121] J. Y. Li and M. L. Dunn, Micromechanics of Magnetoelectroelastic Composite Materials: Average Field and Effective Behavior, *J. Intel. Mater. Syst. Struct.*, vol. 9, pp. 404–416, 1998.
[122] T. Mori and K. Tanaka, Average Stresses in Matrix and Average Energy of Materials with Misfitting Inclusions, *Acta Metall.*, vol. 21, pp. 571–574, 1973.
[123] J. Aboudi, Micromechanical Analysis of the Fully Coupled Finite Thermoelastic Response of Rubberlike Matrix Composites, *Int. J. Solid Struct.*, vol. 39, pp. 2587–2612, 2002.
[124] J. Aboudi and M.-J. Pindera, High-Fidelity Micromechanical Modeling of Continuously Reinforced Elastic Multiphase Materials Undergoing Finite Deformation, *Math. Mech. Solid*, 2004.
[125] J. Aboudi, Micromechanical Analysis of the Finite Elastic-Viscoplastic Response of Multiphase Composites, *Int. J. Solid Struct.*, vol. 40, pp. 2793–2817, 2003.
[126] M. B. Rubin, An Elastic-Viscoplastic Model Exhibiting Continuity of Solid and Liquid States, *Int. J. Eng. Sci.*, vol. 25, pp. 1175–1191, 1987.